Politecnico di Torino

POLITECNICO DI TORINO

Master's Degree in Mechatronic Engineering

Master's Degree Thesis

Modeling and Simulation of Battery Management System: From Concept to Implementation

Supervisor
Prof. Stefano Alberto MALAN

Candidate
Enrico PISTILLI

Company Tutor
Ing. Angelo BORNEO

October 2024

Abstract

In recent years, there has been a marked increase in the adoption of electric vehicles to reduce CO_2 and pollutant gas emissions produced by conventional internal combustion engine vehicles. However, one of the critical aspects of these vehicles is the energy storage in the battery, which requires constant monitoring to ensure optimal performance and prevent premature damage.

The following work focuses on analyzing and developing an advanced system for monitoring and managing batteries used in electric vehicles. The main objective is to develop a Battery Management System (BMS) model by implementing a battery model consisting of eight modules in series, each of four parallel cells. The BMS plays a critical role in optimizing the performance, safety, and longevity of battery packs.
The research focuses on improving the accuracy of the State of Charge (SoC) and the State of Health (SoH) estimation of the battery, the thermal management to mitigate temperature-related degradation and detect critical operating conditions, such as overvoltage, undervoltage, and overcurrent.
Starting with an introduction to battery technologies, the various functions of the BMS were analyzed, implemented, and tested to check the proper functioning of the battery.

Contents

List of Figures

List of Tables

Acronyms

BMS	Battery Management System
SoC	State of Charge
SoH	State of Health
KF	Kalman Filter
EKF	Extended Kalman Filter
UKF	Unscented Kalman Filter
UT	Unscented Transform
DEKF	Dual Extended Kalman Filter
BEV	Battery Electric Vehicle
EV	Electric Vehicle
PHEV	Plug-in Hybrid Electric Vehicle
FCEV	Fuel Cell Electric Vehicle
HEV	Hybrid Electric Vehicle
ICE	Internal Combustion Engine
ISO	International Organization for Standardization
ASIL	Automotive Safety Integrity Level
IEC	International Electrotechnical Commission
HARA	Hazard Analysis and Risk Assessment
AIS	Abbreviated Injury Scale
AAAM	Association for the Advancement of Automotive Medicine

ECU	Electronic Control Unit
OCV	Open Circuit Voltage
LTV	Linear Time-Varying
PDE	Partial Differential Equations
CC/CV	Constant Current Constant Voltage
EIS	Electrochemical Impedance Spectroscopy
LIB	Lithium Ion Battery
NMC	Nickel Manganese Cobalt

Chapter 1

Introduction

Nowadays, electric mobility is a very important concept. More and more car manufacturers are moving towards electric propulsion to replace Internal Combustion Engines (ICEs). The main reason for this transition is pollutant emissions.
ICE vehicles run on gasoline or diesel engines and use internal combustion engines to burn fuel, generating power to move vehicles. The main problem is that combustion generates harmful gasses like carbon dioxide, nitrogen oxides, and particulate matter as byproducts of burning fossil fuels.
To overcome this problem, car manufacturers are moving towards electric vehicles. There are different types of electric vehicles such as Battery Electric Vehicles (BEV), Hybrid Electric Vehicles (HEV), Plug-in Hybrid Electric Vehicles (PHEV), and Fuel Cell Electric Vehicles (FCEV) which are gaining popularity in the transportation sector [5].

Focusing on BEVs, the goal is to produce zero tailpipe emissions, offering a cleaner alternative if the electricity to recharge batteries comes from renewable sources. BEVs operate by utilizing electric power stored in a rechargeable battery pack to propel the vehicle, indeed battery is the primary source of energy for these vehicles. However, storing the energy in a battery represents a key aspect, which must be constantly monitored to ensure optimal performance and avoid premature damage. To achieve these goals, the Battery Management System (BMS) are developed. These last ones use sensors to measure current, voltage, and temperature and control algorithms to balance the charge between cells and protect the battery from dangerous conditions to improve not only the lifetime of the battery but also the safety of the vehicle and passengers.

This master's thesis aims to explore in depth the functioning of a battery and the role of BMS in the automotive sector, analyzing existing technologies, technical challenges, and prospects. The research is organized into different sections: at the beginning, a general overview of the functioning of batteries and the various

technologies used will be given. In particular, a focus will be on the fundamental parameters and the different chemistries and geometries of a battery.
Subsequently, a summary of the functional safety of electrical and electronic systems in production automobiles will be done. Specifically, the first four parts of ISO 26262 will be analyzed, where definitions of Automotive Safety Integrity Level (ASIL), hazards, and risks are given.
A further section will focus on the algorithms and issues that still limit the effectiveness of the BMS, such as accuracy in estimating the State of Charge (SoC) and State of Health (SoH) of the battery, and safety in extreme conditions.
In Chapter 3, the implemented model of the BMS is presented, analyzing the methodology used for each function, and then in Chapter 4 the whole model is tested and the results are shown. Concluding remarks obtained from this Thesis will be drawn in Chapter 5, and promising new research lines that emerge from this work will be outlined as well.

Chapter 2

State of Art

2.1 Battery Technologies

Battery technologies represent a key concept in the renewable energy environment, significantly influencing the efficiency and viability of energy solutions. Designing a battery means choosing its chemistry and geometry. The main technologies used today include lead-acid batteries, nickel-cadmium (NiCd) batteries, sodium-nickel chloride (Na-$NiCL_2$) batteries, and lithium ions. Specific key parameters such as capacity, energy density, cycle life, cost, and environmental impact distinguish each of these technologies.

The capacity of a battery represents the total amount of electricity it can store, measured in ampere-hours (Ah). It is directly related to the energy the battery can provide and therefore determines the range a vehicle can travel on a single charge, meaning a battery with a larger capacity can provide a longer range on a single charge, whereas a lower-capacity battery provides a shorter range.
Capacity can also be measured in watt-hours (Wh), which represents the total energy capacity of a battery after taking into account voltage and current. It is obtained by multiplying the battery voltage (expressed in Volts) by its capacity (in Ah), as shown in the equation (2.1).

$$\text{Energy Capacity [Wh]} = \text{Voltage [V]} \times \text{Capacity [Ah]} \tag{2.1}$$

Specifically, the voltage measures the potential difference between the positive and negative terminals of a battery and it is usually measured in volts (V). It also determines the voltage at which current is driven through the vehicle electrical system and directly affects the battery power output. The battery pack voltage can vary according to a variety of factors, including vehicle design, type of battery used, and required performance characteristics.

The other two important parameters are the energy density and the power density. The first refers to the energy stored per unit volume or mass and it is usually measured in Watt-hours per liter (Wh/L) or Watt-hours per kilogram (Wh/kg). Higher energy density batteries can store more energy in the same volume or weight, allowing for greater range or smaller battery size and weight for a given amount of energy. The second, power density, is a key factor in battery electric vehicle performance because it determines the rate at which the battery delivers energy per unit volume or mass to the vehicle electric motor. Usually measured in watts per liter (W/L) or watts per kilogram (W/kg). Higher power density batteries can deliver more instantaneous power, resulting in improved acceleration, performance, and vehicle responsiveness.
The power density is closely related to the ability of the battery to deliver high current without overheating or voltage drop. Factors such as battery chemistry, electrode materials, battery design, cooling systems, and thermal management play a vital role in determining a battery power density.

As regards the cycle life of a battery, it refers to the number of charge and discharge cycles it can undergo before its capacity drops to a certain level. This is a key factor in the long-term durability and reliability of battery packs for pure electric vehicles. Batteries that last longer, require fewer replacements, and provide better value in the long run.

Furthermore, the charge rate of a battery is the rate at which it can be charged using electrical energy from an external source, usually measured in kilowatts (kW) or miles of additional driving range per hour of charge (mph). Faster charging speeds can reduce the time required to recharge the battery, providing greater convenience for owners of pure electric vehicles, especially during long trips or emergencies.
However, for reliability reasons, the operating temperature range must be monitored. The temperature range defines the temperatures at which the battery can safely and effectively operate, including conditions for charging and discharging. Batteries must maintain optimal temperatures to ensure performance, efficiency, and longevity while avoiding damage or safety hazards as a result of extreme temperatures.

Returning to the various chemical compositions of batteries, the lead-acid battery is the oldest technology. It is very popular because of its low cost and low maintenance requirements ([6], [7]). It has no memory effect, i.e. loss of capacity due to the battery being recharged repeatedly after being only partially discharged. Unfortunately, it has some disadvantages that do not allow it to be used for battery pack applications. These are the low energy density (30-50 Wh/kg) and the fact that it can only withstand a limited number of discharge cycles (500-1000 cycles) from fully charged to fully discharged battery. Furthermore, the presence of lead

does not make this battery pack the best solution in terms of environmental impact. Lead-acid batteries were initially replaced by Ni-MH batteries, which have a higher energy density (40-110 Wh/kg) and are environmentally friendly. However, these batteries also have their drawbacks, which are poor cold performance, memory effects, long battery recharge time, and a high self-discharge rate when idle [5]. The memory effect in batteries is a phenomenon in which the battery appears to "remember" its previous state of charge and consequently exhibits a reduced capacity. It occurs when a battery is repeatedly charged and discharged only partially, rather than fully cycling through its entire capacity.

The nickel-cadmium (NiCd) battery is widely used, especially in applications where long life, low cost, and high discharge rate are important. It can easily withstand rigorous working conditions without compromising the integrity of the cell. The energy density (60-80 Wh/kg) is slightly higher than that of the lead-acid solution but unfortunately has the so-called memory effect. Again, the metals used are highly toxic.

The sodium-nickel chloride (Na-$NiCL_2$) batteries are also known as ZEBRA (Zero Emission Battery Research Activities) batteries. They can use almost all abilities without negatively affecting their lifespan. In addition, the energy contained in the battery is approximately 150 Wh/kg. As a storage source, ZEBRA batteries are a good example. Because the battery is intrinsically safe through a chemical reaction, multiple tests, including immersion in 900 liters of salt water with a salinity of 5%, seismic and vibration testing, and a 30-minute external fire test, did not show damage to the module or battery. The risk of fire is low. It is therefore suitable for stationary energy storage. Due to its discharge duration, the technology is ideally suited for load balancing, voltage management, time shifting, and reduction of fluctuation in power from renewable energy sources [5].

The Lithium ion (Li-ion) battery represents the best technology currently available on the market. It guarantees a significantly higher energy density (118-250 Wh/kg) than other solutions, providing an excellent solution in applications where weight is the main objective. Furthermore, it has no memory effect and can be recharged many times and at any state of charge without impacting its overall capacity. In addition, Lithium-Ion Batteries (LIB) are characterized by a low self-discharge rate and higher voltage compared to other rechargeable batteries. The cost is higher than the other solutions and requires a protection circuit in order not to ruin its performance.
Although lithium ion batteries have limitations and considerations, such as the risk of thermal runaway, susceptibility to overcharging and over-discharging, and possible degradation over time due to factors like high temperatures and cycling,

their performance and lifespan can be significantly improved through proper management and use, including proper charging practices and temperature control. Ongoing research and development efforts are also dedicated to improving the energy density, safety, and longevity of lithium-ion battery technology.

In conclusion, another important design parameter is the geometry of the cells. The battery incorporates the three standard forms of electric vehicle cells, which are cylindrical, pouch, and prismatic cells, as shown in Figure 2.1.

Figure 2.1: Cell geometries

The most typical shape used is cylindrical. It provides good mechanical stability and low cost as it is easy to manufacture. However, the cylindrical shape does not offer high efficiency from the point of view of space utilization because there are air gaps between the cells. This is countered by its high energy density and the fact that the space between the cells can be used for cooling purposes.
Prismatic cells have an aluminum or steel cover to ensure mechanical stability. They provide better space utilization than cylindrical ones. However, such batteries tend to swell due to the formation of a gas inside the cell. For this reason, additional space must be considered when designing the battery pack. They typically have a shorter lifespan than cylindrical cells.
The pouch geometry is typical of the Li-po (Lithium polymer) battery. The main difference is the exterior aluminum-plastic composite film cover, which is flexible. The absence of a hard case makes this a lightweight solution. The space used is more efficient, but the problem of swelling is even more emphasized. Again, space must be left for bulges during the design phase.

2.2 ISO 26262

Over the years vehicles are no longer self-standing mechanical entities driven by persons, but we are moving from mechanical to electro-mechanical paths. In the beginning, electrical parts played a marginal role and were used mainly for illumination, user information, battery charging, starter, and ignition, while mechanical components were responsible for torque generation, distribution, and controlling dynamic vehicle behavior.
However, the demand for improved performance and new features grew significantly and the limit of what was possible using only mechanical components was reached. As a result, electrical and electronic components were massively introduced to overcome this limit. Today, the electronic part dominates the mechanical part and more than 50% of the cost of developing a vehicle comes from the design and validation of the electrical part.
Nevertheless, electronic equipment can lead to issues relevant to the user's safety caused by the interaction among electronic systems during their operations, unsafe situations caused by the incorrect behavior of a system in an unpredicted situation, failure with safety-relevant consequences, and reasonably foreseeable misuse. For these reasons, ISO 26262 has been introduced.
ISO 26262 is the international standard for the functional safety of automotive electrical and electronic systems, and it is the adaptation of the IEC 61508 series of standards to address the sector-specific needs of Electrical and Electronic (E/E) systems within road vehicles. (Part 1 of [8])
Functional safety is a part of overall system safety and is defined as the absence of unreasonable risk (of injuries) due to hazards caused by malfunctioning behaviors of Electrical and Electronic systems (random and systematic faults).
The standard provides guidance and requirements for the development of safety-critical automotive systems to ensure that they meet specific safety standards throughout their life cycle. It also applies to all electrical and electronic safety-related systems in the automotive industry, including their components, software, and processes.
Regarding the structure of ISO 26262, it is divided into ten parts, as depicted in the Figure 2.2, each covering different aspects of functional safety in automotive systems. They are:

- Part 1: Vocabulary;
- Part 2: Management of Functional Safety;
- Part 3: Concept Phase;
- Part 4: Product Development at the System Level;
- Part 5: Product Development at the Hardware Level;

- Part 6: Product Development at the Software Level;
- Part 7: Production and Operation;
- Part 8: Supporting Processes;
- Part 9: Automotive Safety Integrity Level (ASIL)-oriented and Safety-Oriented Analysis;
- Part 10: Guidelines on ISO 26262.

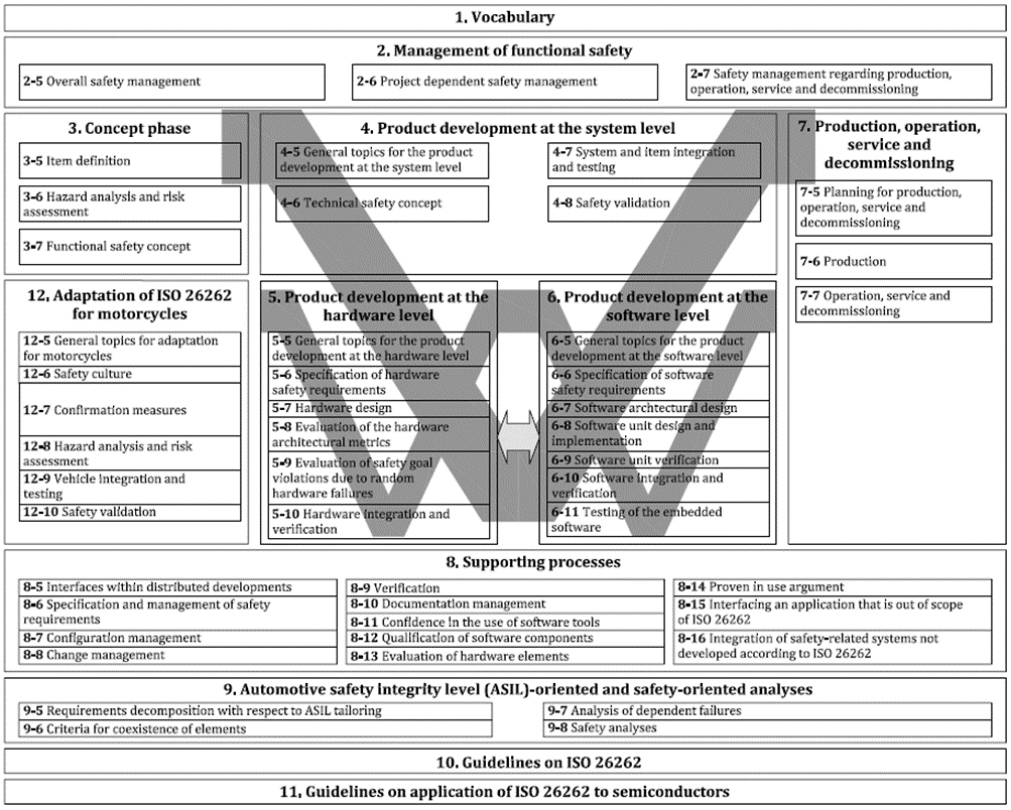

Figure 2.2: Overview of the ISO 26262 series of standards

In the first part, formal definitions of fault, failure, error, and malfunction are given. All the other terms used in the definition of the other parts of the standard are also introduced in the form of a glossary, to limit possible ambiguities.
Part 2 of ISO 26262 focuses on the management of functional safety. It provides information on overall safety management, project-dependent safety management, and safety management with respect to production, operation, service, and decommissioning. It defines the requirements and activities for the safety lifecycle of a product, from the concept phase to the decommissioning phase. It also specifies

the roles and responsibilities of the involved parties, such as the project manager, the safety manager, the safety engineer, and the independent assessor. Part 2 of ISO 26262 aims to ensure that the safety goals and requirements are identified, implemented, verified, and maintained throughout the product development process. ISO 26262 defines an automotive-specific risk-based approach to determine integrity levels, that is ASIL (Automotive Safety Integrity Levels). There are four ASIL levels: ASIL A (lowest) to ASIL D (highest). The classification helps determine the level of rigor required for safety processes and the allocation of resources for safety-related activities. ASILs are used to specify which of the requirements of ISO 26262 are applicable to avoid an unreasonable residual risk. ASIL level is determined using a Hazard Analysis and Risk Assessment (HARA) method to recognize hazardous events in the system and to indicate safety goals that mitigate the hazards ([9], [10]). To choose the correct level, the severity, exposure, and controllability criteria that are taken into account in Part 3 of the standard must be considered.
The Severity is an estimate of the amount of damage caused to one or more persons that may occur during a potentially dangerous event, i.e. considering damage to the driver, passengers, and others outside the vehicle. The severity in ISO 26262 is categorized in levels, as shown in Figure 2.3. For example, when the severity class is S0 means that the hazard analysis and risk assessment determine that the consequences of the malfunctioning behavior of the item are clearly limited to material damage, so ASIL is not required. (Part 3 of [8])

	Class			
	S0	**S1**	**S2**	**S3**
Description	No injuries	Light and moderate injuries	Severe and life-threatening injuries (survival probable)	Life-threatening injuries (survival uncertain), fatal injuries

Figure 2.3: Classes of Severity

Estimation of severity class can also be carried out by referring to the Abbreviated Injury Scale (AIS) classification provided by the Association for the Advancement of Automotive Medicine (AAAM) as illustrated in Figure 2.4, which classifies in seven levels the extent of physical injury in an accident:

- AIS 0: no injuries;
- AIS 1: light injuries such as skin-deep wounds, muscle pains, whiplash, etc.;
- AIS 2: moderate injuries such as deep flesh wounds, concussion with up to 15 minutes of unconsciousness, uncomplicated long bone fractures, uncomplicated rib fractures, etc.;
- AIS 3: severe but not life-threatening injuries such as skull fractures without brain injury, spinal dislocations below the fourth cervical vertebra without

damage to the spinal cord, more than one fractured rib without paradoxical breathing, etc.;

- AIS 4: severe injuries (life-threatening, survival probable) such as concussion with or without skull fractures with up to 12 hours of unconsciousness, paradoxical breathing;
- AIS 5: critical injuries (life-threatening, survival uncertain) such as spinal fractures below the fourth cervical vertebra with damage to the spinal cord, intestinal tears, cardiac tears, more than 12 hours of unconsciousness including intracranial bleeding;
- AIS 6: extremely critical or fatal injuries such as fractures of the cervical vertebrae above the third cervical vertebra with damage to the spinal cord, extremely critical open wounds of body cavities (thoracic and abdominal cavities), etc. (part 3 of [8])

	Class of severity (see Table 1)			
	S0	**S1**	**S2**	**S3**
Description	No injuries	Light and moderate injuries	Severe and life-threatening injuries (survival probable)	Life-threatening injuries (survival uncertain), fatal injuries
Reference for single injuries (from AIS scale)	AIS 0 and less than 10 % probability of AIS 1-6; or damage that cannot be classified safety-related	More than 10 % probability of AIS 1-6 (and not S2 or S3)	More than 10 % probability of AIS 3-6 (and not S3)	More than 10 % probability of AIS 5-6

Figure 2.4: Classes of severity considering AIS classification

As regards the probability of exposure, it can be traced back to an operational situation that may be hazardous if it coincides with the failure mode under analysis. The probability of exposure can be viewed in terms of the frequency of exposure or the duration of exposure. There are five classes of exposure, as shown in Figure 2.5, and when the exposure probability falls within E0, it does not require ASIL assignment.

	Class				
	E0	**E1**	**E2**	**E3**	**E4**
Description	Incredible	Very low probability	Low probability	Medium probability	High probability

Figure 2.5: Classes of probability of exposure regarding operational situations

Controllability is the ability to avoid a given damage through the timely reactions of those involved, possibly with the support of external measures. Reasonably

foreseeable improper actions (such as failure to keep a safe distance) should be taken into account in the analysis of the controllability parameter. There exist four different classes of controllability, as illustrated in Figure 2.6, and again if C0, it does not require the determination of ASIL.

	Class			
	C0	C1	C2	C3
Description	Controllable in general	Simply controllable	Normally controllable	Difficult to control or uncontrollable

Figure 2.6: Classes of controllability

ASIL level is determined for each hazardous event based on severity, probability of exposure, and controllability in accordance with the table in Figure 2.7:

Severity class	Exposure class	Controllability class		
		C1	C2	C3
S1	E1	QM	QM	QM
	E2	QM	QM	QM
	E3	QM	QM	A
	E4	QM	A	B
S2	E1	QM	QM	QM
	E2	QM	QM	A
	E3	QM	A	B
	E4	A	B	C
S3	E1	QM	QM	A[a]
	E2	QM	A	B
	E3	A	B	C
	E4	B	C	D

Figure 2.7: ASIL levels determination

In addition to the four ASILs, it is introduced the class QM (Quality Management) which indicates that the quality processes are sufficient to manage the identified risk.
In addition, part 3 of ISO 26262 also gives a definition of "item", which is a "system or combination of systems to which the standard is applied, that implements a function or part of a function at the vehicle level" (part 1 of [8]) within the scope of functional safety. The term "item" is referred to various entities such as sensors and actuators, software components, Electronic Control Units (ECUs), and all the other entities that help in identifying, analyzing, and addressing potential hazards and risks.
Part 4 of the standard focuses on product development at the system level starting with developing the technical safety concept. This last one "is an aggregation of the technical safety requirements and the corresponding system architectural design that provides a rationale as to why the system architectural design is suitable to

fulfill safety requirements resulting from activities described in ISO 26262-3 (with consideration of non-safety requirements) and design constraints" (part 4 of [8]). The product development activities in Part 4 interact with other parts of the ISO 26262 standard, particularly Parts 3 (Concept Phase), 5 (Product Development at the Hardware Level), and 6 (Product Development at the Software Level), as shown in Figure 2.8.

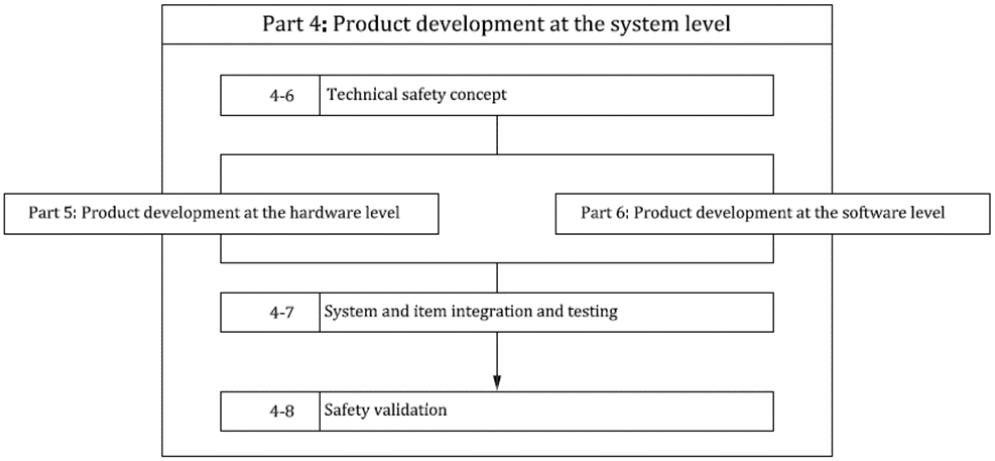

Figure 2.8: Reference phase model for the development of a safety-related item

Regarding system and item integration and testing, the integration steps are defined for all levels of integration, starting from hardware and software of an element and verification to vehicle integration and verification.
The last concept introduced is safety validation, which is the final step in the development of the system product. It "provides evidence of appropriateness for the intended use and aims to confirm the adequacy of the safety measures for a class or set of vehicles. Safety validation assures that the safety goals have been achieved, based on examination and test" (part 4 of [8]). The validation of safety goals is applied to the integrated item at the vehicle level, and the validation plan includes test procedures for each safety goal with a pass/fail criterion.

2.3 Battery Management System

With the development of electric vehicles, the battery has become the most prominent energy storage device. Over the years, battery technology has grown very quickly as a result of the increasing demand for more efficient performance. Cells with higher power and energy densities have been developed, but also regulations due to safety are increasing and becoming more stringent. For these reasons, it is equally important to improve the performance of the Battery Management System (BMS) to ensure safety, high efficiency, reliability, and cost-efficient solutions and

to extend the battery life ([11], [12]). The need to have a control system mainly comes from the newer chemistry used for realizing batteries. Indeed, nowadays, Lithium-Ion Batteries (LIB) are used due to their higher power and energy density, lower self-discharge, and higher voltage per single cell. However, LIBs are very delicate cells that need to work within a precise range of both voltage and temperature. The key functions of BMS are:

- Cell Monitoring;
- State of Charge (SoC) Estimation;
- State of Health (SoH) Estimation;
- Thermal Management;
- Cell Balancing;
- Battery Safety and Protection;

2.3.1 Cell Monitoring

The aim of the BMS is monitoring and control. Considering the first, Cell Monitoring plays an important role. It must monitor the voltage, current, and temperature of each cell. The voltage must be monitored to ensure that it remains within safe limits during the charging, discharging, and idle state. In case of over-voltage or under-voltage conditions, which indicate cell imbalance or potential failure, the BMS must take corrective action to prevent damage. As regards the current, it measures the current flowing in and out of each cell to prevent overcharging or over-discharging, which can lead to a degradation of the cell performance and lifespan. In addition, Cell Monitoring must measure the temperature of the cell by using sensors that are placed strategically within the battery pack. High temperature can indicate overcharging, high current, or thermal runaway that must be avoided. In these cases, the BMS must adjust the charging rates or activate the cooling systems as needed to maintain safe temperatures. All the information taken from the Cell Monitoring is used to estimate the State of Charge (SoC) of the battery [13].

2.3.2 State of Charge Estimation

Knowing SoC is very important because it allows to determine how far the vehicle can travel on the current charge and so defining the range estimation, allows also to assess the battery degradation and health and optimize charging and discharging. In theory, the state of charge is defined as the ratio between the residual capacity, C_r, and the total capacity, C_t:

$$\text{SoC} = \frac{C_r}{C_t} \tag{2.2}$$

However, the direct determination of the SOC of a battery is a very complex task, so there exist different methods used to estimate it and they are:

- Voltage-Based estimation;
- Coulomb Counting;
- Kalman Filtering;
- Model-based estimation;
- Neural network.

1. **Voltage-Based estimation** aims to determine the remaining capacity of the battery using a discharge test. Using a discharge curve, in which the voltage is plotted against the SoC, the voltage method allows determining the SoC by reading the battery voltage. However, voltage readings are significantly affected by the current of the battery as a result of the electrochemical kinetics of the battery and temperature. To make this method more accurate, the voltage reading can be compensated by a correction term proportional to the battery current and by using a lookup table of the Open Circuit Voltage (OCV) vs. temperature, where the OCV of a battery is the voltage measured when the battery is in a steady state in an open circuit condition. However, the necessity for a consistent voltage range for batteries and the long time required complicates the implementation of the voltage method ([13], [14]).

2. The **Coulomb Counting** method is also known as the Ampere hour (Ah) integration method. Its goal is to estimate the state of charge of the battery by accumulating the electricity charged or discharged when the battery is charged and discharged. This method can be described in the equation (2.3):

$$\mathrm{SoC}(t) = \mathrm{SoC}(t_0) + \eta \int_{t_0}^{t} \frac{I(\tau)}{C_n}\, d\tau \tag{2.3}$$

   where $\mathrm{SoC}(t_0)$ is the known initial SoC, $I(\tau)$ is the current value which is positive for charging and negative for discharging, η stands for the efficiency of battery charging or discharge, and C_n is the nominal capacity of the battery. The coulomb counting method has its advantages and drawbacks. As regards the firsts, the charging and discharging current can be easily measured and the results achievable can be very precise. However, due to the losses during charging and discharging, the releasable charge is always less than the stored charge and in addition to the self-discharging, cause accumulating errors. Besides, the a priori knowledge of the initial values of the State of Charge, $\mathrm{SoC}(t_0)$, obtained by the lookup table of the OCV characteristic, becomes the challenging issue [1].

3. The **Kalman filter** method is a mathematical algorithm used to estimate the state of a dynamic system based on measurements affected by noise over time. In the context of battery management, the Kalman filter can be applied to estimate the state of charge (SoC) of a battery by integrating measurements of voltage, current, and temperature. Indeed, the Kalman filter is applied by considering each cell to be a dynamic system and by considering as input the current and the temperature of the cell and as output the terminal voltage.
   The Kalman filter is very effective for linear systems, whereas it requires a linearization for nonlinear systems to approximate them as Linear Time-Varying Systems (LTV). This last one is then used in the Kalman filter, and the entire process constitutes the Extended Kalman Filter (EKF) which is used in various algorithms to estimate the state of lithium batteries. The advantage of using the Kalman filter to estimate SoC is the ability to handle uncertainties and noise in measurements and to provide accurate state estimates even in the presence of modeling errors or disturbances. However, to use the Kalman filter, the battery behavior must be known to develop a mathematical model.

4. **Model-based** methods are very flexible and can be adapted to different chemistries, configurations, and operating conditions. These methods rely on mathematical models that describe the relationship between external inputs such as current, voltage, and temperature, and internal state variables such as the State of Charge (SoC). The goodness of the estimate depends on the accuracy of the model used, and in the literature, there exist many: electrochemical, mathematical, and equivalent electrical models.
   The electrochemical model is based on the computation of Partial Differential Equations (PDEs) that describe battery dynamics linking macroscopic parameters such as voltage and current to microscopic ones related to chemical reactions inside the cell. The method has the potential to be very accurate, but due to the heavy computation, it is unusable for those applications in which high-speed calculation is required.
   Mathematical models are used in very specific situations. In these models, the measured voltage and current are used to determine coefficients of mathematical and statistical functions that have little connection to battery physics.
   In the equivalent electrical models, to estimate the state of charge of the battery, it must be first derived a circuit model that replicates the dynamics of the battery. In this case, in the literature, there are different kinds of equivalent circuits, but all have something in common, like the use of lumped components such as resistors, capacitors, and voltage sources. Specifically, resistors represent the internal resistance of the battery, which causes voltage drop during charge and discharge, and capacitors represent the battery capacitance, which accounts for the charge storage capability and voltage source, whose aim is to represent the OCV.

The most common equivalent circuit is the equivalent Thevenin model or RC model, shown in Figure 2.9, which is composed of a series of RC branches, that model the internal dynamics of the battery [15].

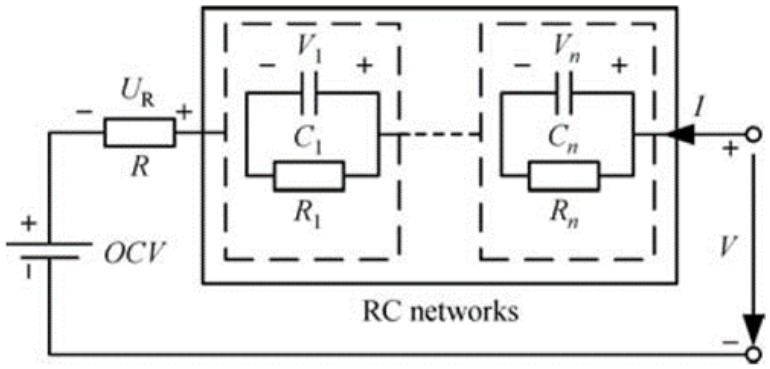

Figure 2.9: Equivalent circuit of a battery cell ([1])

The number of RC branches tells the order of the model. The simplest model can be obtained using just one branch, and it is called the first-order RC model. The last one allows us to model the behavior of the battery exhaustively.

5. The **Neural network** is composed of three layers, as shown in Figure 2.10. The input layer takes the vector of the voltage, current, and temperature, the hidden layer, and the output layer are the state of charge of the battery. This method is used when it is necessary to process a huge amount of data and it is very robust concerning noise and disturbances. Consequently, the estimation of the SOC with a Neural network is accurate and precise.

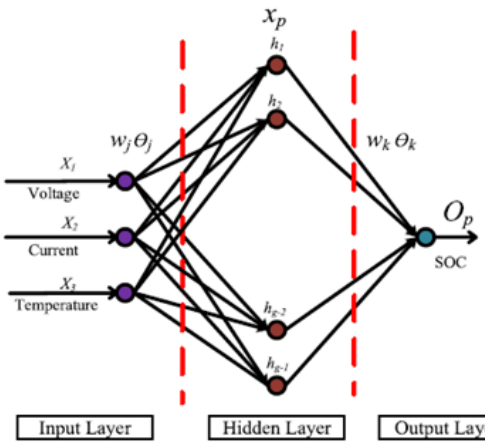

Figure 2.10: The general architecture of the 3-layer Neural network structure [2]

2.3.3 State of Health estimation

The State of Health (SoH) is a very important parameter that must be monitored to maximize battery life and ensure reliable battery performance. Batteries lose capacity over time, meaning that they can hold less and less power, and SoH helps track this degradation by predicting the number of times the battery can be charged and discharged before its life is up [11], and managing battery performance accordingly [16].
The State of Health can be defined as the ratio between the maximum capacity that the battery can deliver and the nominal capacity, as shown in equation (2.4):

$$SoH = \frac{C_{\max}}{C_n} \tag{2.4}$$

At first, it is useful to understand that SoH is influenced by some factors like:

- Cycle Life, every time a battery undergoes a charge-discharge cycle, the overall capacity and performance decrease;
- Operating conditions, the health of a battery is influenced by the temperature which can accelerate the degradation of the performance of a battery. For example, for a Li-ion battery, the optimal working range of temperature is between -20° C and +60° C;
- Charge and discharge rates, because charging or discharging the battery too quickly can generate excess heat which leads to degradation.
- Ageing, batteries degrade over time due to chemical reactions within the cells, and, in addition, there is also a reduction of chemical components inside the batteries which leads to a reduction of the effectiveness of the internal reactions;
- Maintenance helps preserve the state of health of a battery. Maintenance also includes regular charging cycles and avoiding overcharging or deep discharging.

However, SoH is not a parameter that can be directly measured, so it requires a method that allows one to estimate the state of health [17]. SoH estimation techniques can be divided into two different groups, capacity estimation and internal resistance estimation. The firsts aim to estimate the aging of the battery considering the degradation of the capacity, whereas the second considers the value of the internal resistance that increases with time [18].
Capacity estimation techniques group different types of methods like the model-based observers, inference-based techniques, Constant Current Constant Voltage (CC/CV) approach, geometric approach, pulsed discharge approach, and curve fitting approach [19].
In model-based observers, as in the estimation of the SoC, the goal is to use an

equivalent model to estimate the capacity of the battery. The main models used are the electrochemical model and the equivalent RC circuit model. In the electrochemical model, chemical reactions play the main role and are used to model the behavior of the battery. The electrochemical model is based on the computation of Partial Differential Equations (PDEs), but to simplify the calculations, PDEs are reduced into differentiation equations. This method aims to estimate the capacity degradation of the battery to estimate the state of health.
The equivalent RC circuit model is based on realizing a circuit with a series of RC branches to represent the behavior of the battery. This model aims to estimate the capacity of the battery using an observer. For this reason, the Kalman filter technique is strictly connected due to the iterative process that reduces the estimation error to zero. When more than one Kalman filter is used, we can refer to the Extended Kalman Filter (EKF), Dual Extended Kalman Filter (DEKF), or Unscented Kalman Filter (UKF).
Inference-based techniques involve deriving predictions about the battery health based on observed data and models. Typically, statistical inference, mathematical models, or machine learning algorithms are used.
The Constant Current Constant Voltage (CC/CV) approach aims to estimate the capacity of the battery as the sum of the product of the current sent into the battery and the sampling time [18].
The geometric approach is based on the analysis of the charge/discharge curves of a battery. The voltage is plotted against the state of charge, and the geometric properties of these curves are examined to infer the degradation of the battery capacity over time. Four features are considered: the area under the CV curve, the time duration of the CV curve, the maximum radius of curvature of the CV stage, and the slope of the voltage drop at the beginning of the discharge curve.
The pulsed discharge approach is a technique used to estimate the capacity of a battery by drawing short current pulses and analyzing its voltage response. By comparing the predicted SoH with the actual capacity, the health condition of the battery can be assessed.
The curve fitting approach involves fitting curves to the capacity, the number of cycles, and the voltage versus State of Charge (SoC) data collected during battery charging and discharging.
In internal resistance estimation techniques, there are two main methods, Electrochemical Impedance Spectroscopy (EIS) and model-based observers. The first involves applying a small AC signal to the battery, changing the frequency of it, and then measuring the resulting voltage using a potentiostat or impedance analyzer. The voltage and current are used to estimate the value of the internal resistance, which is the ratio of voltage to current.
In the model-based observer techniques, mathematical models of the battery behavior are employed. The main two models are the electrochemical and the RC equivalent circuit model. In the electrochemical model of the battery, an increase

in the internal resistance of the battery is observed. The rise in impedance results from the diminishing concentration of lithium ions and the thickening of the solid electrolyte interface layer. As regards the RC equivalent circuit model, the internal resistance is estimated by using observers like the Kalman Filter.

2.3.4 Thermal Management

As mentioned, temperature is a crucial parameter in the operation of a battery to maintain its performance, safety, and longevity. In fact, the BMS has the objective of controlling the overall temperature of the battery, also considering the ambient temperature, and keeping it at the optimal point under different operating conditions [11].
Thermal management systems have the goal of determining the temperature of the battery and controlling the cooling or heating mechanism accordingly. The problem is related to the determination of the internal temperature of the cell. The surface temperature can be easily measured using thermal sensors or thermocouples, whereas the internal temperature can be measured by injecting a sensor inside the cell. However, this method requires expensive sensors and is a tricky method. For these reasons, in general, sensors are strategically placed throughout the battery pack to monitor the temperature of a single cell or a group of cells [1].

2.3.5 Cell balancing

A battery is composed of cells that can be put in parallel or series to satisfy the requirements of voltage and energy. The BMS continuously monitors the voltages of each cell, identifying overcharged and undercharged ones. Variations due to differences in cell chemistry or operating conditions can occur and the efficiency of the battery pack can be compromised if there is a mismatch between the voltage and capacity of the connected battery cells ([11], [20]). For example, during discharging, if a cell runs out of charge the discharge stops even though other cells still hold charge.
Cell balancing aims to equalize the voltages of the cells without overcharging and over-discharging and adjusting the currents to achieve optimal cell voltages. There are two main types of cell balancing: passive and active. The firsts are very simple and economical to set up, necessitating solely a controlled switch and a bleeding resistor in each cell. With this configuration, energy is drawn from the most charged cell and dissipated as heat [11].
In active balancing, charge is transferred between cells using switches, capacitors, inductors, or DC-DC converters to redistribute energy and equalize cell voltages. Different active balancing techniques exist depending on the amount of energy that must be redistributed. This method is more complex and expensive, but more efficient, enabling faster and more precise balancing.

2.3.6 Battery Safety and Protection

Due to the chemistry of the battery, hazardous conditions could be caused. Harmful conditions could be deep charging of the battery, overcharging of the battery when it is fully charged, charging or discharging the battery with a high C-rate that overcomes the safe level, or short circuits that can occur accidentally. The BMS also sets safety limits for the operating temperature, to prevent overheating, which can lead to thermal runaway and catastrophic failure.
For these reasons, the charging process of the battery pack must be regulated by the BMS to ensure safe and efficient operation. The charging rate depends on the customer's request, but batteries have limitations due to the chemistry and structures that must be also considered in the realization of charging stations or charging devices [11].

Chapter 3

Software Development

In the following chapter, the implemented model, as shown in Figure 3.1, will be thoroughly analyzed and described in detail.

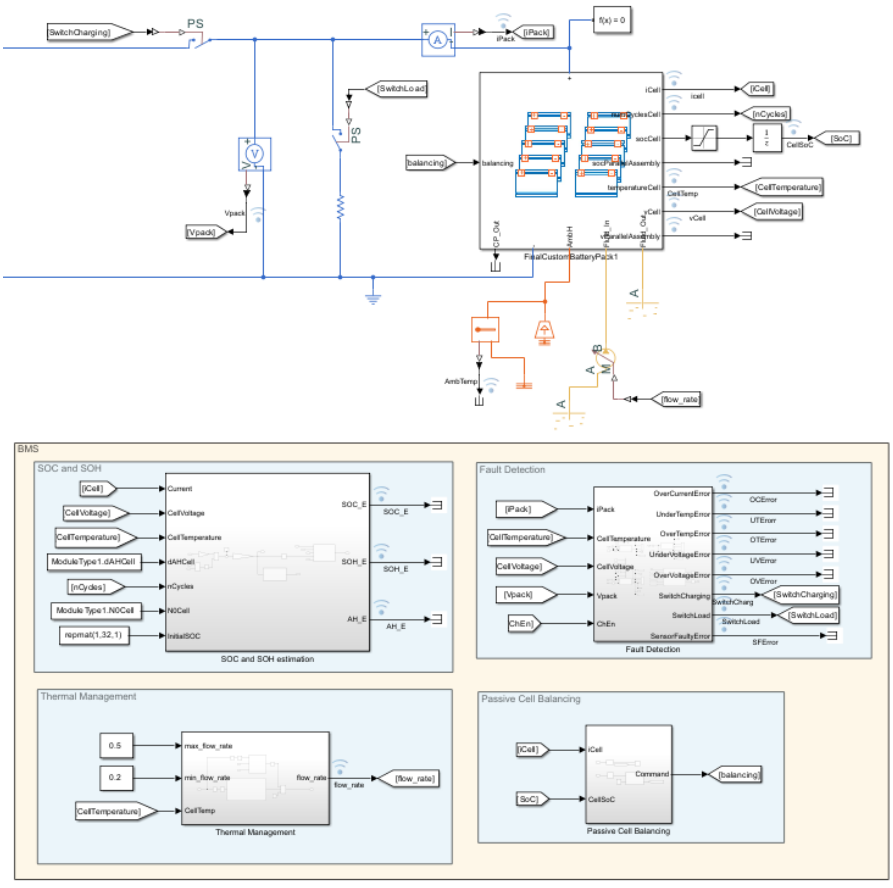

Figure 3.1: Complete Simulink model

The model is divided into two key sections: the battery pack, which is depicted in the upper part of the figure, and the various functions of the Battery Management System (BMS). The battery pack section represents the physical and electrical characteristics of the battery cells and modules, while the BMS functions encompass a range of control and monitoring operations, such as state estimation, thermal management, and protection mechanisms, ensuring safe and efficient battery operation.

3.1 Battery Pack

The first step is to create a battery pack model that could handle a small vehicle. The battery pack is a collection of individual cells connected in series and/or in parallel to achieve the desired voltage and capacity value. Today, there are various types of cells on the market, which vary from each other in terms of chemistry, size, shape, and performance.
Among the various cell solutions available, a cell with high energy density and robust performance characteristics was selected. Specifically, the Samsung SDI 3.7V 94Ah NMC Prismatic Battery Cell is selected [3] due to the Nickel Manganese Cobalt (NMC) chemistry, which is a powerful solution that provides a combination of energy capacity, thermal stability, and cycle life. Furthermore, the prismatic shape facilitates optimal space utilization and modular design, which allows the realization of a battery pack that is both compact and capable of delivering high power output. The chosen cell is shown in Figure 3.2.

Figure 3.2: Samsung SDI 3.7V 94Ah NMC Prismatic Battery Cell [3]

The next step is to implement the selected cell, with its characteristics, within MATLAB/Simulink, the environment in which the various functions of the BMS will be implemented and the battery pack will be tested.
To do so, “Battery Builder” is used, which is a set of tools and features within

the MATLAB environment, particularly in the Simulink and Simscape libraries, designed to model, simulate, and analyze battery systems [21].
Battery Builder allows one to insert, easily and intuitively, all the characteristics of the cell, starting from the geometry and its dimensions, up to the technical information regarding mass, capacity, and energy. According to its datasheet, the parameters of the chosen cell have been collected in the Table 3.1:

Height	125 mm
Length	173 mm
Thickness	43 mm
Mass	2.1 kg
Capacity	94 Ah
Nominal voltage	3.68 V
Total energy	345 Wh
Recommend Charging Constant Current	72 A
Charging Upper Limit Voltage	4.15 V
Max Continuous Discharge Current	150 A
Discharging Cut-off Voltage	2.7 V
Minimum Temperature	-20°C
Maximum Temperature	65°C

Table 3.1: Parameters of the cell

In addition, Battery Builder allows for the definition of conditional parameters that control the visibility of component members within the cell block, including parameters, variables, nodes, inputs, and outputs. In particular, the model can account for:

- **Temperature dependence and thermal effects**, which indicates that the model accounts for the influence of temperature on battery performance and heat generation and dissipation.
- **Aging of the Open Circuit Voltage (OCV)**, which is crucial for understanding long-term battery behavior.
- **Degradation of the battery capacity over time**, reflecting the reduction in charge the battery can hold as it ages.
- **Increase in internal resistance** as the battery ages, affecting its efficiency and thermal performance.
- **Capacity fade**, representing the gradual loss of capacity.

Subsequently, a parallel assembly consisting of four cells is realized. When cells are connected in parallel, all positive and negative terminals are connected, which

impacts the total capacity of the system, which is equal to the sum of the capacities of the individual cells, thus achieving a total capacity of 376 Ah. The parallel assembly realized is illustrated in Figure 3.3.

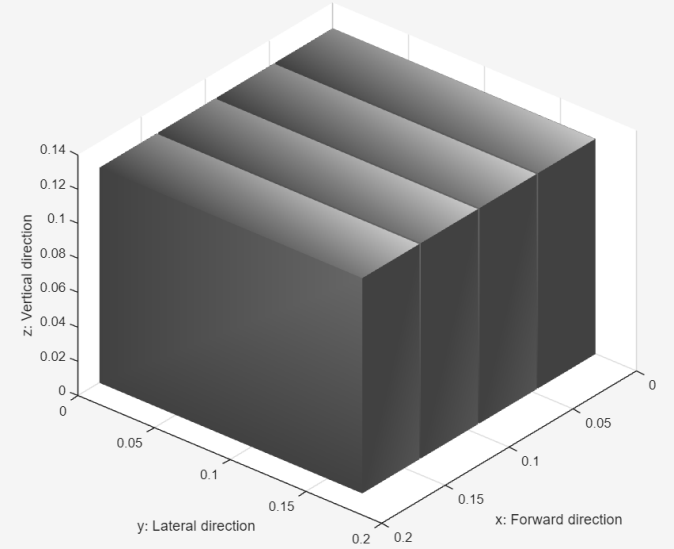

Figure 3.3: Parallel Assembly

This type of connection is particularly useful when a higher energy reserve is needed without increasing the system voltage, translating to a longer operating time for the system before recharging is required.
At this point, through some editable settings in Battery Builder, the battery pack is designed with a focus on detailed modeling, including thermal consideration. Specifically, a passive balancing strategy is chosen, meaning the pack relies on internal balancing mechanisms rather than external controls.
Regarding the thermal options for this battery pack, active cooling is specified, with a defined thermal resistance in the coolant thermal path. This resistance governs the efficiency of heat transfer from the battery cells to the coolant and the external environment.

Proceeding with the implementation of the battery pack, the module still needs to be implemented. To combine the effects of both series and parallel configurations, providing a high voltage output with a significant capacity, eight parallel assemblies are connected in series as shown in Figure 3.4. To summarize the characteristics of the battery, a 4p8s configuration has been implemented. In this configuration, four cells are connected in parallel within each series group, which increases the total capacity while maintaining the voltage unchanged. Additionally, eight parallel groups are connected in series, which increases the total voltage of the battery pack up to 29.6 V.

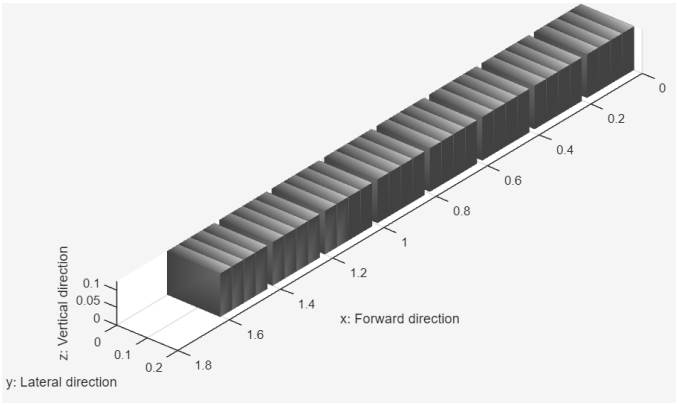

Figure 3.4: Battery Pack

Furthermore, to optimize the thermal management, it is designed the cooling plate for the battery pack. To address this challenge, U-shaped channels have been chosen for the cooling plate block path, which can be quite effective at directing coolant flow and dissipating heat from the battery cells maintaining the thermal stability of the battery system.

In conclusion, after having set all the basic parameters of the battery pack, starting from the cell up to the module, a Simscape block of the pack is generated by Battery Builder, as shown in Figure 3.5.

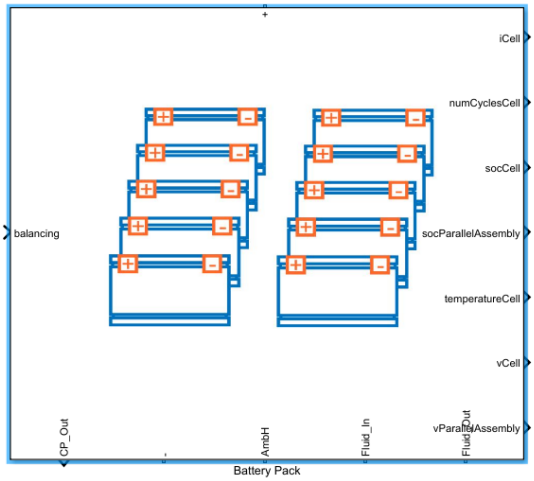

Figure 3.5: Simscape block of the battery pack

The Simscape block represents a detailed and interconnected model of a battery pack. Within the battery pack, each cell is modeled as an equivalent circuit

comprising voltage and resistance elements that represent the dynamic of the cell behavior under different conditions.
Understand how this block works, it is essential to focus on its inputs and outputs, which facilitate the connection of the battery to a circuit, allowing it to be monitored and controlled in practice.
First of all, the model includes **positive (+) and negative (-) input ports**, which represent the electrical connection to the battery, through which current flows.
In addition to primary power connections, the model has an input port for **balancing**, which is crucial to equalizing the State of Charge (SoC) of each cell at the same level. Proceeding, the model includes outputs related to individual cell monitoring, which are:

- The **iCell** port gives information about the current flowing through each cell.
- The **numCyclesCell** port tracks the number of charge-discharge cycles of each cell, providing information on the cell aging process.
- The **socCell** port gives as output the State of Charge (SoC) of each cell, offering a real-time view of the remaining energy.
- The **temperatureCell** port monitors the temperature of each cell.
- The **vCell** port gives the voltage of each cell.

The model also considers the behavior of groups of cells through the **socParallelAssembly** and **vParallelAssembly** ports, which track the State of Charge and voltage of entire parallel assemblies of cells. Finally, some ports simulate the flow of cooling fluid through the battery pack, namely the **Fluid In** and **Fluid Out** ports, as well as the **AmbH** port, which refers to the ambient temperature around the battery pack.

3.2 SoC and SoH estimation

Subsequently, after the battery pack implementation was complete, the focus was shifted to the implementation of the basic functions of the BMS. The first step is the development of an algorithm for estimating the State of Charge (SoC) and the State of Health (SoH) of the battery cells. The implemented model is depicted in Figure 3.6.

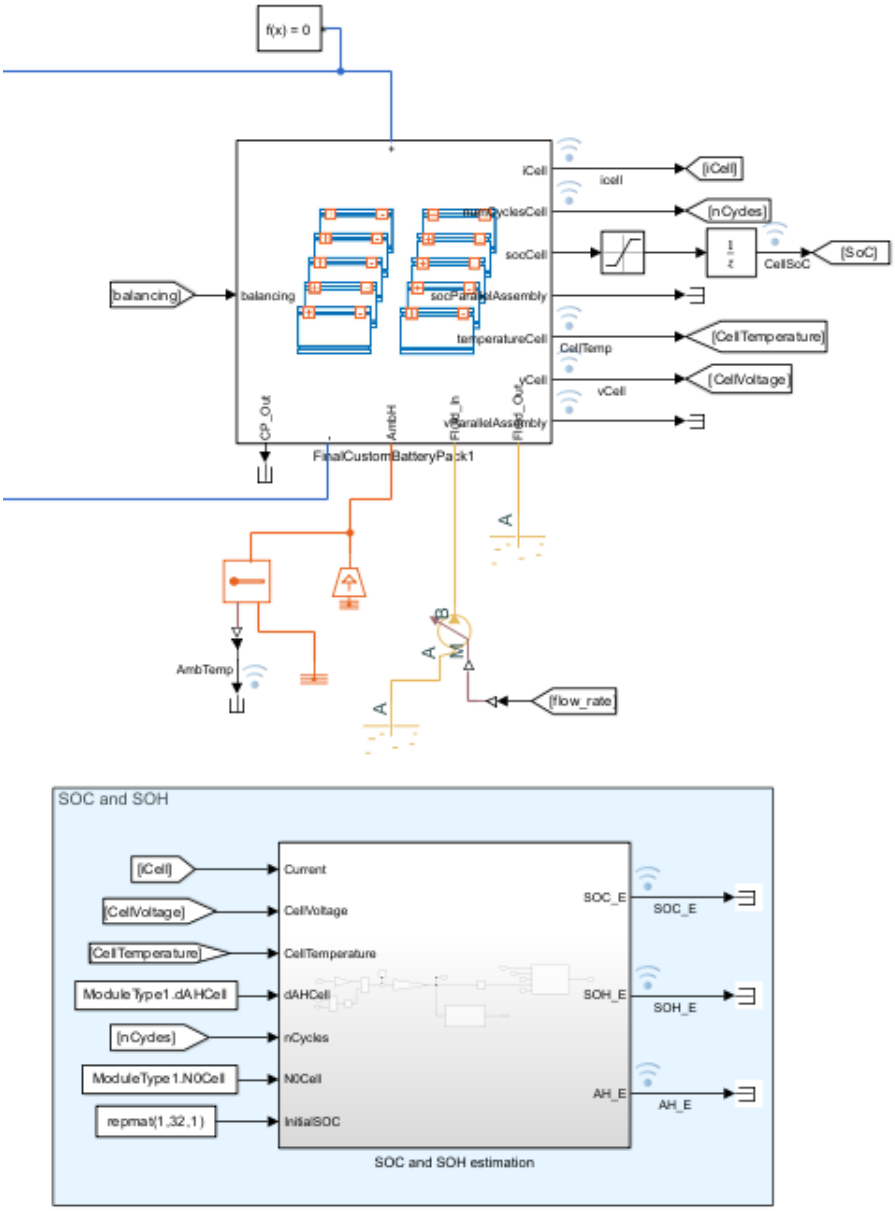

Figure 3.6: Simulink model of the SoC and SoH estimation

Exploring the subsystem of the SoC and SoH Estimator, for both two functions, a pre-existing block in the Simulink library is used, which uses, among other inputs, cell capacity. Capacity fading is included to obtain more accurate estimates of SoC and SoH in order to realize a model similar to that of a real battery.
Capacity fading is a phenomenon that directly affects the estimation of the SoC and SoH, as the actual battery capacity decreases over time, due to various chemical and physical degradation factors. If fading is excluded, there is a risk of overestimating

the SoC and SoH values of the cells.

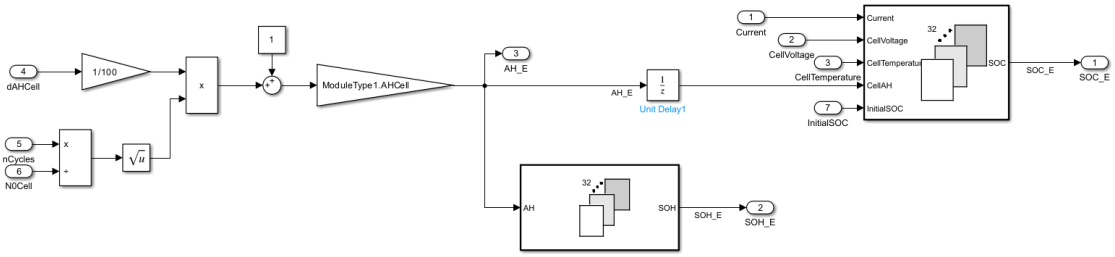

Figure 3.7: SoC and SoH estimation subsystem

As shown in Figure 3.7, in the first part of the model there is the representation of the equation that governs the capacity fading [22]. The equation is displayed in (3.1).

$$q_{\text{nom,fade}} = q_{\text{nom}} \left(1 + \frac{\delta_{AH}}{100}\sqrt{\frac{n}{N}}\right) \tag{3.1}$$

where q_{nom} is the nominal capacity, from which state of charge is calculated, δ_{AH} is the change in cell capacity after N discharge cycles, which is always negative due to the inevitable degradation and reduction in the capacity of the cell over time, and n is the actual number of cycles which comes out from the battery as "numCyclesCell".
Regarding the SoC Estimator block, it estimates the SoC based on an Unscented Kalman Filter (UKF). This last one is an improved version of the traditional Kalman Filter (KF) because is an algorithm designed for nonlinear state estimation. In contrast to the Extended Kalman Filter (EKF), which linearizes the system based on the current estimate, the UKF utilizes the Unscented Transform (UT) to represent the mean and covariance of the state distribution accurately.
Specifically, the UKF utilizes a set of sample points known as sigma points to represent the mean and covariance of the state distribution. When these propagated sigma points move through the nonlinear system, they also capture the posterior mean and covariance of the state distribution. This approach allows the UKF to reflect more faithfully the underlying dynamics of the system, making it effective in scenarios where precise estimation is crucial, such as in BMS to evaluate the SoC ([23], [24], [25]).

Analyzing the SoC Estimator block, shown in Figure 3.8, it estimates the SoC by taking in multiple inputs that are:

- the current flowing through the cells, **iCell**;
- the voltage of each cell, **CellVoltage**;

- the temperature of the cells, **CellTemperature**;
- the capacity of the cells, **CellAH**;
- the initial value of SoC, **InitialSOC**.

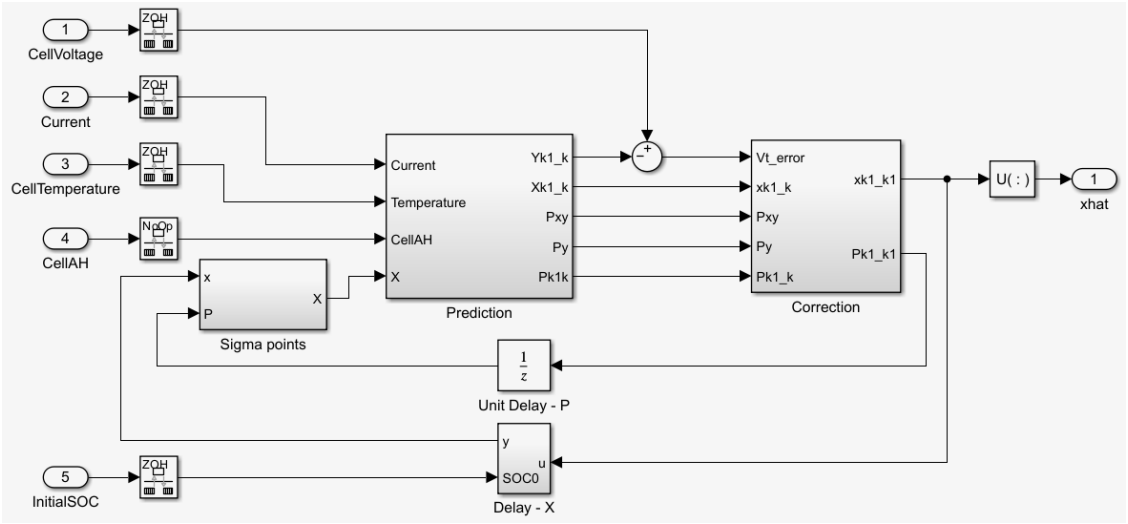

Figure 3.8: Simulink model of the SoC Estimator block

Specifically, the block processes all the inputs through an algorithm to continuously update the SoC of each cell. The UKF algorithm starts with an initial guess of the SoC, provided as one of the inputs under **InitialSOC**, which for this model is chosen to be equal to 1 for all the cells. Considering the current state of the battery as described by the current, voltage, temperature, and known capacity, and based on the previous state estimate, the UKF predicts the SoC.

As said before, the UKF uses a mathematical model that captures the non-linear dynamics of the battery, predicting how much the SoC should decrease given a certain current drain, considering voltage response and temperature effects.
In particular, the SoC Estimator block, generates the so-called sigma points that represent the distribution of possible states. Passing these points through the nonlinear model, the distribution of the next state (SoC) is predicted.
Furthermore, the UKF compares the predicted voltage from the state model with the actual measured cells voltage coming directly from the battery block. This comparison helps adjust the prediction based on real data and allows the filter to adjust the sigma points, improving the SoC estimation by giving more weight to the predictions that align closely with the measurements.
Finally, using the adjusted sigma points, the UKF produces a new estimate for the

SoC which is used as the basis for the next prediction.

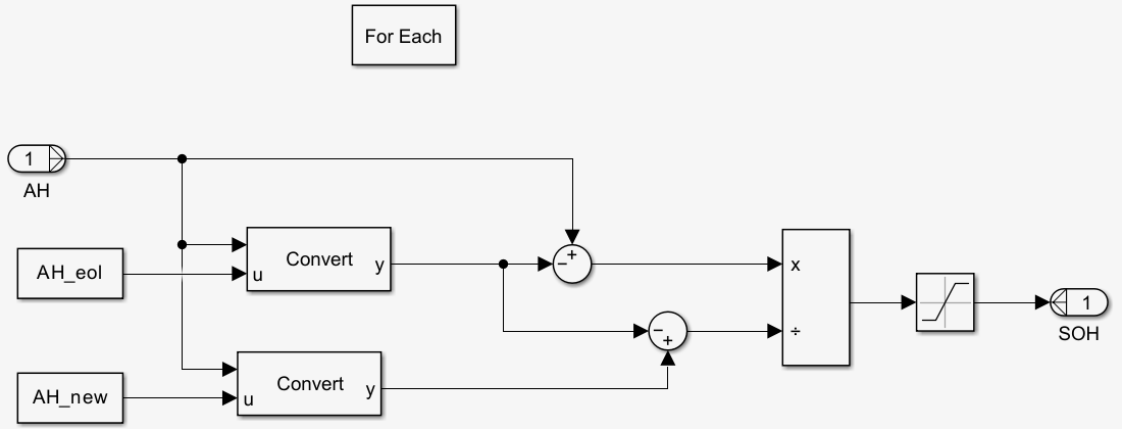

Figure 3.9: Simulink model of the SoH Estimator block

The SoH Estimator block, illustrated in Figure 3.9, is designed to estimate the State of Health of a battery using as the only input the capacity of the cells, expressed in AH. This input is critical as it reflects the current capacity of the battery relative to its designed capacity. The functioning of the block primarily relies on capacity fade, which directly alters the capacity, thereby affecting the SoH of the battery.
The SoH Estimator block computes the State of Health of the battery as a function of the only input, which is the cell capacity Q, as shown in equation (3.2):

$$SoH_Q = \frac{Q - Q_{\text{eol}}}{Q_{\text{col}} - Q_{\text{new}}} \tag{3.2}$$

where Q_{eol} represents the cell capacity when the battery is at the end of its life, and Q_{new} is the cells capacity when the battery is new.

3.3 Thermal Management

Thermal Management aims to ensure the safety, efficiency, and longevity of the battery pack, indeed the main role is to prevent the battery from overheating, which can lead to degradation, reduced performance, and thermal runaway and fires.
To achieve this goal, an active cooling system is developed as can be seen in Figure 3.10:

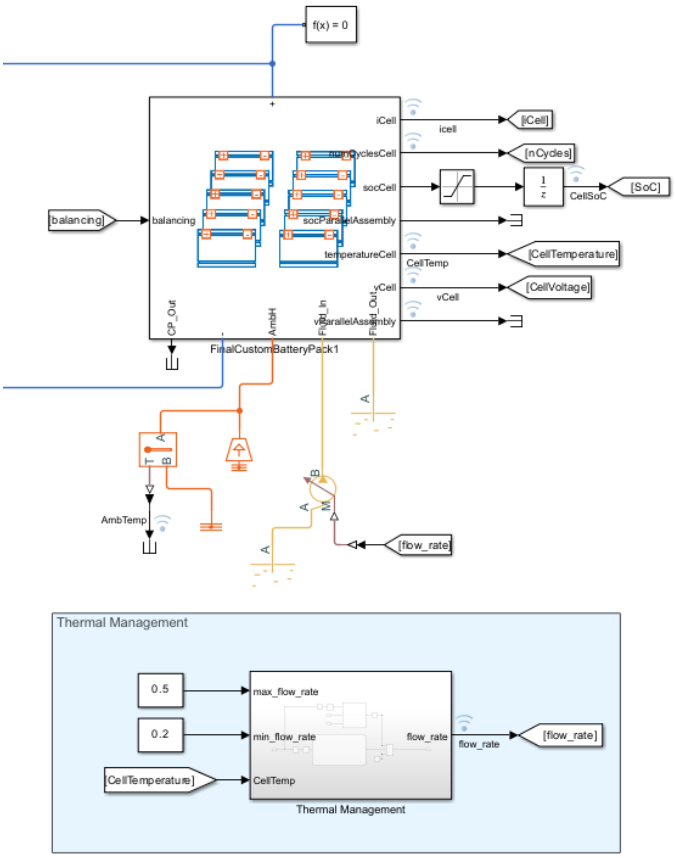

Figure 3.10: Simulink model of the Thermal Management

Focusing on the Thermal Management subsystem, it has three inputs:

- **max_flow_rate**, which is the maximum flow rate of the cooling liquid. It serves as an upper boundary to ensure that the cooling system does not overactivate;
- **min_flow_rate**, which represents the minimum flow rate of the cooling liquid. It ensures that there is always a baseline flow of coolant when the system is activated, preventing any abrupt thermal spikes;
- **CellTemperature**, which comes out directly from the battery and gives real-time information on the temperature of the cells.

Regarding the output, the only parameter is **flow_rate**, which represents the effective flow rate of the cooling liquid. This flow rate is crucial as it determines the amount of coolant passing through the battery system to maintain optimal temperatures. Upon exploring the subsystem, the model appears as shown in Figure 3.11:

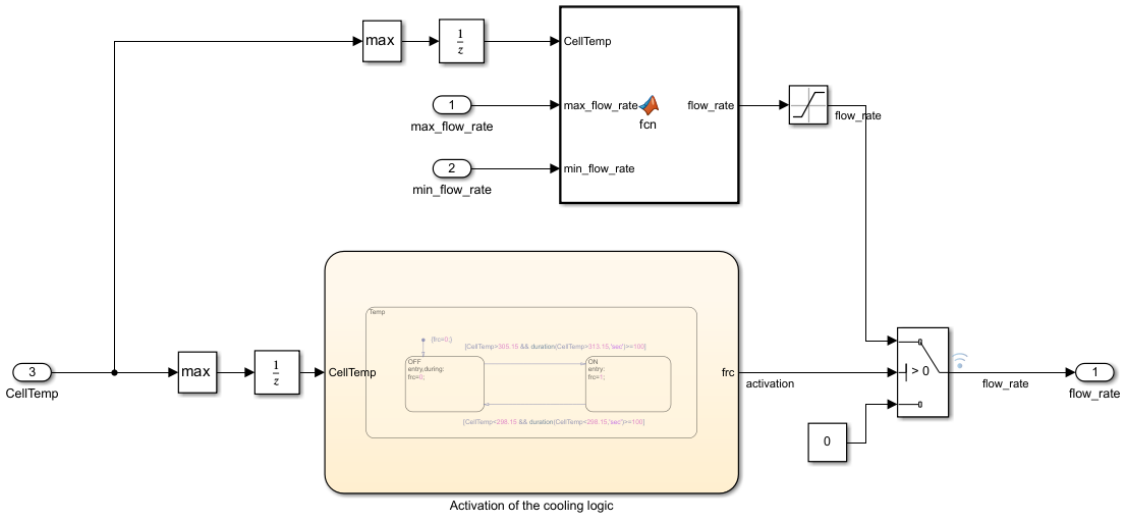

Figure 3.11: Thermal Management subsystem

The subsystem is structured into two parts: the MATLAB function and the Chart. The first is responsible for calculating and generating the effective flow rate, which is essential for maintaining efficient system performance. On the other hand, the chart plays a key role in determining when to activate the cooling logic, ensuring that the system operates within optimal temperature ranges.
Exploring the MATLAB function, it is designed to generate a variable flow rate that adjusts according to the temperature of the cells. Specifically, the function outputs the maximum flow rate when the highest temperature among the cells exceeds 306.15 K (33°C), and it performs a linear interpolation between two predefined values of the flow rates for temperatures ranging between 298.15 K (25°C) and 306.15 K (33°C). This interpolation allows for a gradual and smooth adjustment of the flow rate in response to temperature changes within this range, ensuring precise control and optimal performance of the cooling system.
Proceeding with the Chart, it appears as shown in Figure 3.12:

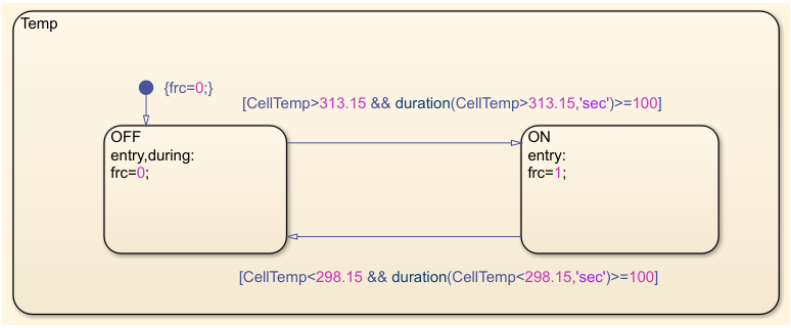

Figure 3.12: Chart of the activation of the cooling

The system has two distinct states: OFF and ON. The OFF state signifies that the cooling system is inactive and not engaged, which means that the battery is not required to be cooled. On the contrary, the ON state indicates that the cooling system is on and actively cooling the battery.
The primary objective of the chart is to generate a binary vector that provides clear logic for activating the cooling system. Specifically, this vector assumes a value equal to 0 when the coolant is off, and so no cooling action, and a value of 1 when the coolant is on.
Transitioning between states in the system is governed by specific conditions. The system will pass from the OFF state to the ON if the highest temperature among the cells is higher than 313.15 K (40°) and remains above this threshold for at least 100 seconds. This condition ensures that the cooling system only activates when the temperature is persistently high, which helps prevent unnecessary cooling cycles. Conversely, the system will pass from the ON state to the OFF state if the cell temperature is lower than 298.15 K (25°C) and stays below for at least 100 seconds. This ensures that the cooling system remains active until the temperature is sufficiently low.

Another important aspect to consider in the model is the Switch (Figure 3.11), which plays a crucial role in controlling the output flow rate based on the activation signal coming from the Chart. This switch functions determining whether the flow rate should be passed through or blocked, depending on the state of the cooling logic.
Specifically, when the activation signal is greater than 0, and so the cooling is active, the switch allows the calculated flow rate to pass through, maintaining the desired temperature within the system.
When the cooling is inactive, meaning the activation signal is 0, the switch automatically sets the flow rate to 0, stopping any flow and preventing unnecessary cooling when it is not required.

Returning to the entire Simulink model of the Thermal Management system depicted in Figure 3.10, a closer examination of the bottom section of the battery pack reveals critical components associated with fluid dynamics and temperature regulation. Indeed, there are two key ports related to the coolant flow management that are **Fluid_in** and **Fluid_out**.
The **Fluid_in** port serves as the entry point for the coolant, which primarily absorbs excess heat generated by the cells during operation, thereby maintaining the battery at an optimal temperature to ensure efficiency and preventing overheating. Then, the warmed coolant will come out from the **Fluid_out** port to be cooled down again in a Reservoir before being recirculated back into the system.
An essential component within the model is the Flow Rate Source, which is connected to the output of the Thermal Management subsystem. This Flow Rate

Source represents an ideal mechanical energy source in a thermal liquid network that can maintain a constant or controlled mass flow rate or volumetric flow rate regardless of the pressure differential. This consistent flow is critical for effective heat transfer, ensuring that the coolant can adequately absorb heat as it passes through the battery cells.

Regarding the **AmbH** port, it is connected to both an ambient Temperature Sensor and a Temperature Source. The sensor continuously monitors the temperature of the environment surrounding the battery pack, which is directly imposed by the Temperature Source, simulating the ambient temperature conditions in the model.

3.4 Passive Cell balancing

In the automotive industry, battery cells are typically connected in series and parallel configurations to achieve the desired high voltage and capacity values. However, this arrangement introduces several practical challenges due to inherent variations among the cells. These variations can arise from manufacturing tolerances, differing self-discharge rates, temperature fluctuations during operation, and uneven aging processes. Over time, these discrepancies tend to worsen, leading to potential imbalances within the battery pack. Such imbalances can result in situations where certain cells are subjected to overload or excessive discharge, both of which can significantly compromise performance, leading to wasted energy and battery safety, as shown in Figure 3.13.

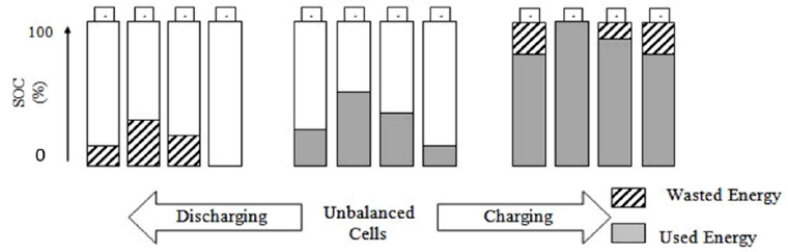

Figure 3.13: Effect of SoC imbalance on a battery pack (4-cell) [4]

It is evident that this nonuniformity not only restricts the overall capacity of the battery but also increases the risk of safety hazards, such as thermal runaway or cell damage. To mitigate these risks and enhance the longevity and reliability of the battery, it is crucial to ensure that all cells within the battery pack remain properly balanced throughout their operational life.
Effective cell balancing is therefore a fundamental aspect of a BMS, as it plays a critical role in optimizing performance, extending the battery life cycle, and

ensuring vehicle safety.

In practice, as said in section 2.3.5 (**Cell balancing**), cell balancing aims to equalize the voltages and State of Charge (SoC) of individual battery cells, especially when they are not uniformly charged [4]. To achieve this objective, a passive cell balancing approach has been chosen for the implemented model as shown in Figure 3.14. Passive cell balancing works by dissipating the extra energy of the more charged cells through resistors, effectively reducing their charge until the charge equals that of the less charged cells within the battery pack. In doing so, the charge of all cells is equalized by ensuring that any surplus energy in the overcharged cells is safely released as heat [4].

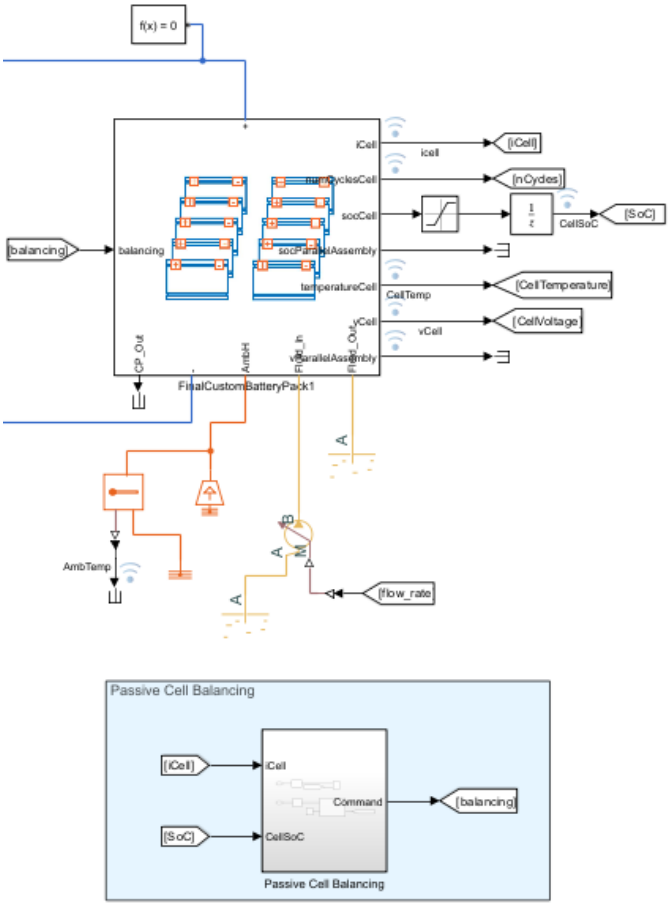

Figure 3.14: Simulink model of the Passive Cell Balancing

Concentrating on the Passive Cell Balancing subsystem, it operates based on two inputs that directly come out from the battery:

- **iCell**, which provides real-time measurements of the current flowing through

each cell, enabling the system to monitor the current status and ensure the balancing process is accurately managed.

- **SoC**, which delivers information regarding the state of charge of each cell, allowing the subsystem to make necessary adjustments to maintain balanced operation across all cells.

The sole output of the subsystem is the **balancing**, which is the command to initiate the passive cell balancing process. Exploring the subsystem it appears as shown in Figure 3.15:

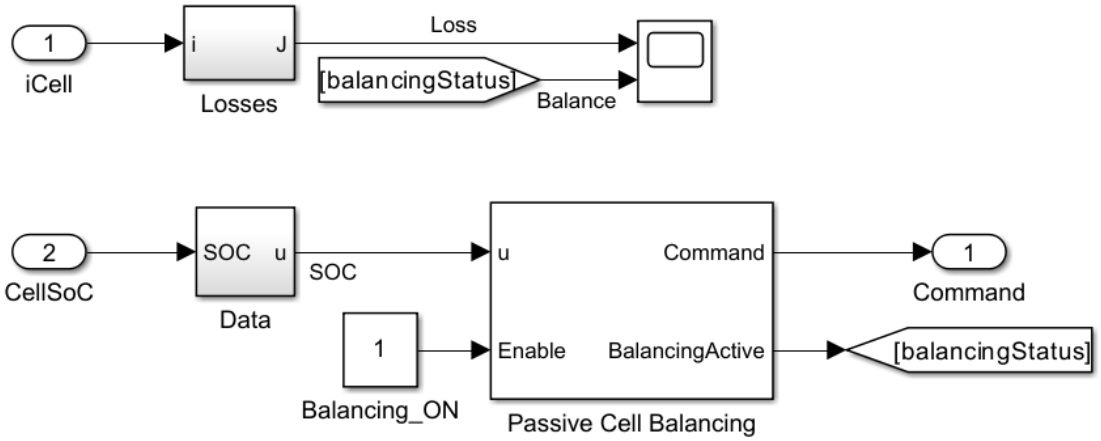

Figure 3.15: Passive Cell Balancing subsystem

The subsystem can be observed to be divided into two parts: the first part, which accounts for the current flowing through the cells, and the second part, which takes into account the State of Charge of the cells.
Focusing on the first part, the current of the cell is fed into a secondary subsystem in which a MATLAB function is present. This function is responsible for calculating the power losses within the system. Specifically, it determines the total power losses by summing up the power dissipated across resistors that are connected to several parallel cells. The power loss for each resistor is computed as the product of the current through the resistor squared and the resistance of the resistor as illustrated in equation (3.3):

$$\text{Pwr} = I^2 \cdot R \tag{3.3}$$

where I represents the current passing through the resistor and R represents the resistance.
In the second part of the subsystem, the State of Charge of the cells is fed into an additional subsystem. Within this subsystem, a MATLAB function is implemented. This last one calculates the average SoC for each parallel assembly

of cells. The estimated average SoC then serves as the input for the subsequent Passive Cell Balancing block, ensuring that the cells within the parallel assembly are balanced according to the computed average State of Charge.

The Passive Cell Balancing block is a pre-existing block that implements an algorithm for cell balancing. It aims to equalize the SoC across cells dissipating excess energy from the more charged cells in a bleed resistor. In practice, the algorithm discharges some of the cells until their state of charge is equal to the State of Charge of the cell with the lowest value. Looking under the mask of the block, the Simulink model is illustrated in Figure 3.16:

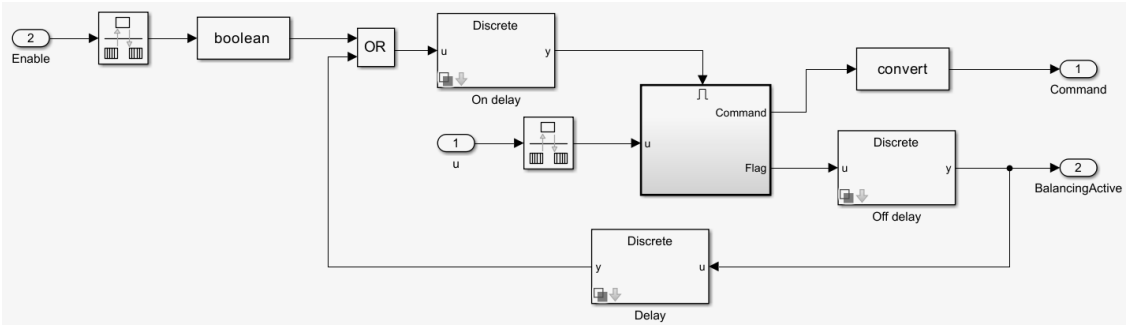

Figure 3.16: Simulink model of Passive Cell Balancing block

Specifically, the block has two inputs: **u**, representing the State of Charge of the cells, and **Enable**, which functions as a trigger for the balancing procedure. The Enable input port is set equal to 1, as illustrated in Figure 3.15. This configuration allows the block to activate the balancing process until the cells within the battery reach a fully balanced state, ensuring that all cells have equalized charge levels.

3.5 Fault Detection

The last function implemented is the fault detection mechanism, illustrated in Figure 3.17. The last is designed to continuously monitor the parameters associated with the battery pack, including current, temperature, and voltage. The primary objective of the Fault Detection function is to identify abnormal conditions that could lead to faults or failures within the battery pack.

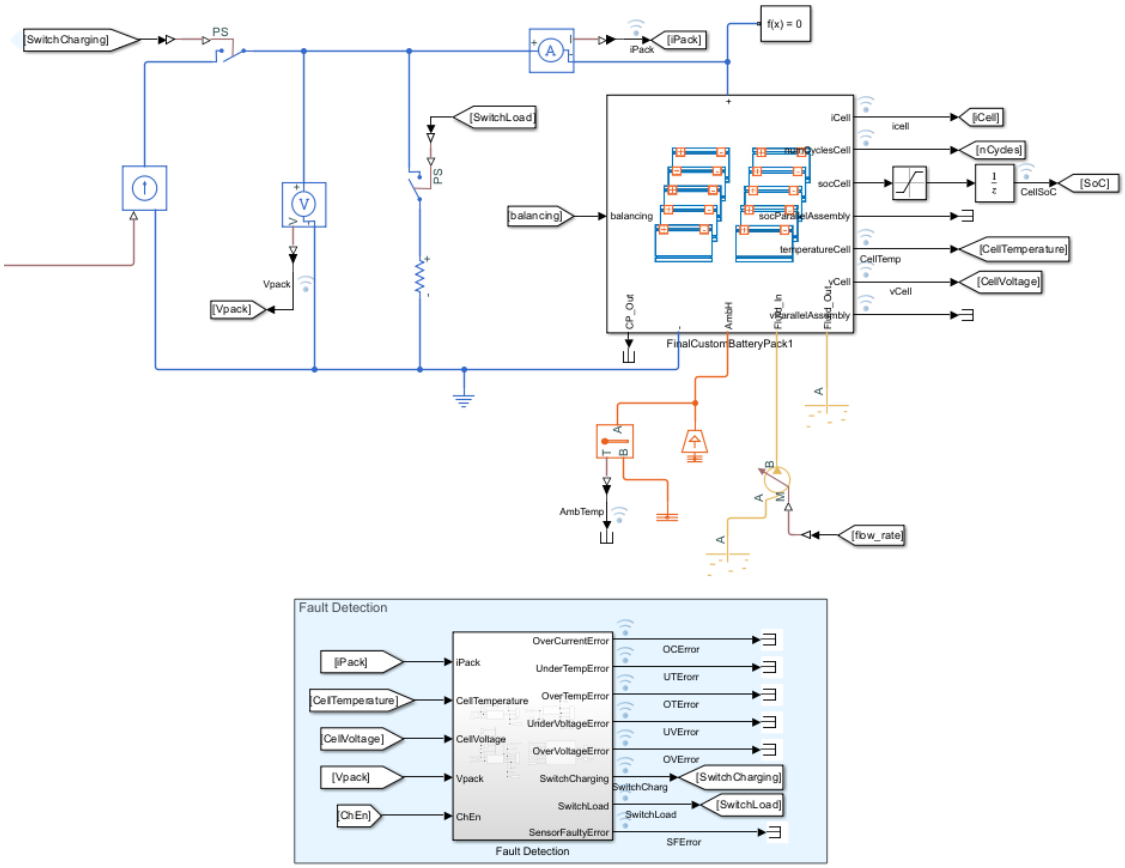

Figure 3.17: Simulink model of Fault Detection

Focusing on the Fault Detection, the subsystem has several inputs:

- **iPack**, the current flowing through the battery pack, which is measured by a Current Sensor block connected in series with the battery;
- **CellTemperature**, which provides real-time measurements of the temperature of each cell;
- **CellVoltage**, which provides the voltage across each cell;
- the voltage of the battery pack, **Vpack**, which is measured thanks to a Voltage Sensor block put in parallel to the battery;
- **ChEn**, which is a binary signal with two values of 1 and 0 depending on whether the battery is in charging mode or not.

Regarding the output of the subsystem, six binary signals play a crucial role in detecting potential errors within the system. These signals serve as indicators of specific fault conditions. The binary signals are the following:

- **OverCurrentError**: this signal will assume a value equal to 1 when the current flowing through the system exceeds the predefined safe limit, indicating an overcurrent condition.

- **UnderTempError**: this signal is activated when the temperature of the battery cells falls below the minimum safe operating threshold.

- **OverTempError**: this signal will be equal to 1 when there is a potential overheating issue. It occurs when the temperature of the battery cells exceeds the maximum allowable limit.

- **UnderVoltageError**: this signal indicates that the voltage of the battery cells has dropped below the minimum safe level, which may suggest excessive discharge or a fault within the battery cells.

- **OverVoltageError**: this signal is activated when the voltage across the battery cells exceeds the maximum safe limit, indicating a potential overcharging condition.

- **SensorFaultyError**: this signal is triggered when a malfunction or abnormality is detected in one of the sensors that monitor the battery parameters.

In addition to these Fault Detection outputs, there are other two binary signals designed to control two key switches within the circuit.
The first binary signal, **SwitchCharging**, is responsible for controlling the switch connected to the charging circuit. When the signal is activated (set to 1), it enables the charging circuit, allowing the battery to be charged. Conversely, when the signal is deactivated (set to 0), it disconnects the charging circuit, effectively preventing the battery from being charged. This control mechanism is crucial to ensure that the battery is charged only under safe conditions, as dictated by the system fault detection algorithms.
The second binary signal, **SwitchLoad**, controls the switch that connects the battery to the load. When this signal is activated, the load is connected to the battery, allowing the battery to discharge. If the signal is deactivated, the load is disconnected from the battery, preventing further discharge.

Upon exploring the Fault Detection subsystem, it appears as shown in Figure 3.18.

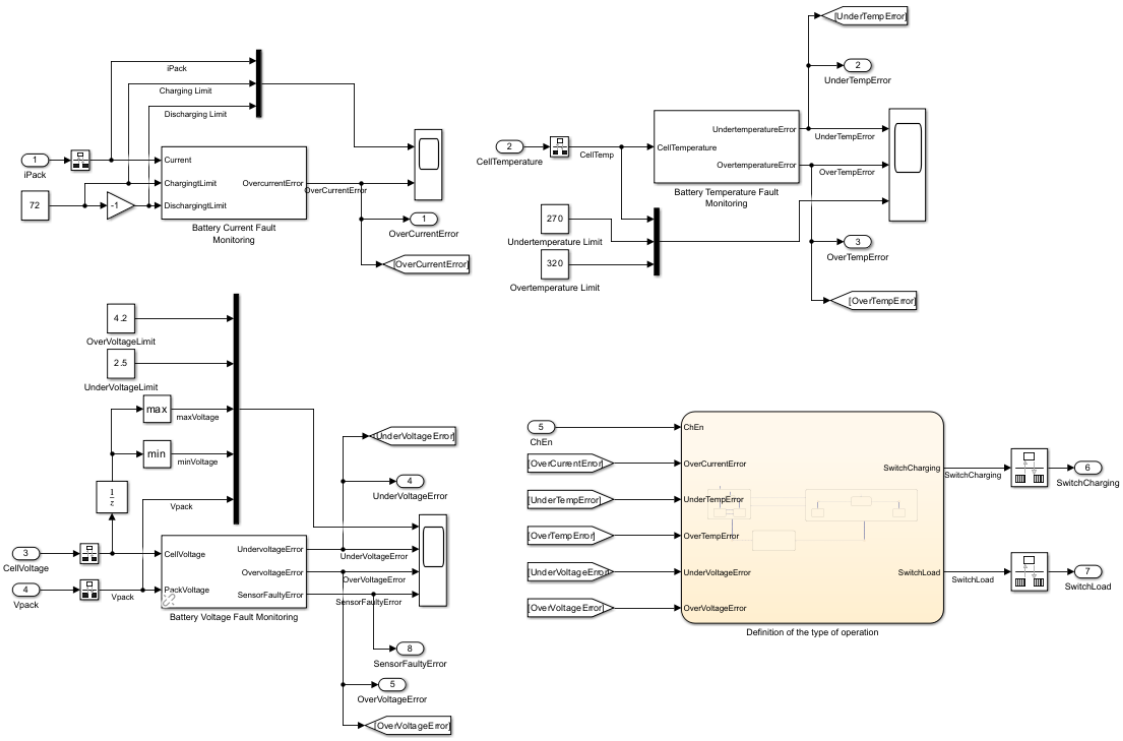

Figure 3.18: Fault Detection subsystem

The subsystem is composed of three pre-existing blocks and a Chart. These three blocks implement the main functions essential for effective Fault Detection which are:

1. The **Battery Current Monitoring** is responsible for continuously measuring and analyzing the current flowing through the battery. The aim is to keep the current remaining within safe operating limits. Specifically, if an over-current condition is detected, this block will trigger signaling a potential fault.

2. The **Battery Voltage Monitoring** monitors the voltage across the battery pack. The block detects conditions where the voltage may drop below or rise above the predefined safe thresholds. In the event of under-voltage or over-voltage conditions, this block generates error signals to prevent scenarios such as excessive discharge or overcharging.

3. The **Battery Temperature Monitoring** is responsible for monitoring the temperature of the battery cells. This block has the role of ensuring that the battery operates within the safe temperature range, [270,320] K, by detecting both under-temperature and over-temperature conditions.

In addition to these three blocks, the subsystem includes a state Chart that implements the logic of Fault Detection and directly manages the operation of the

two switches. The Chart is responsible for choosing when and how the switches, **SwitchCharging** and **SwitchLoad**, should be opened or closed based on real-time conditions. Looking inside the chart, it appears as illustrated in Figure 3.19. This Chart is composed of three main different states and transitions that represent different operational modes of the system, such as normal operation, fault condition, and permanent fault. Each state is linked to specific actions that directly impact the status of the switches.

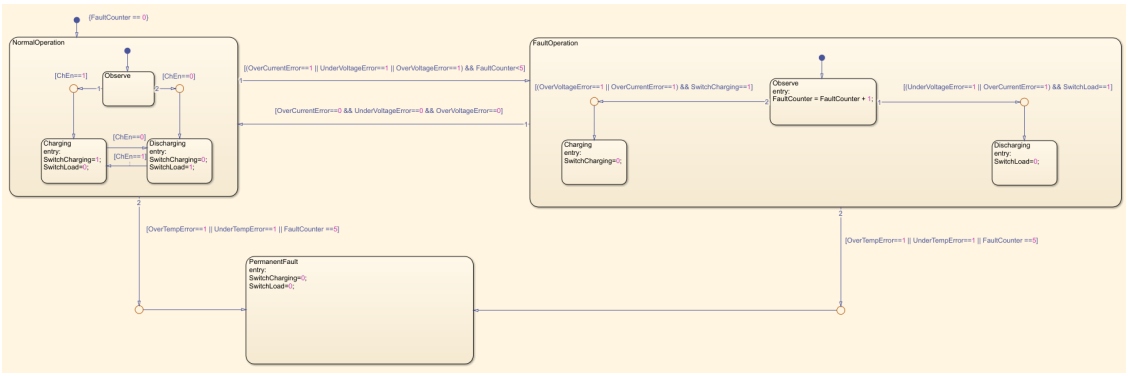

Figure 3.19: Chart of the definition of the type of operation

The **NormalOperation** is the initial state where the system operates without any detected faults. Inside the state, a sub-chart determines whether the battery is in charging mode (ChEn==1) or discharging mode (ChEn==0). Specifically, in charging mode the **SwitchCharging** is set to 1, allowing the battery to charge, while the **SwitchLoad** is set to 0, disconnecting the load. Conversely, in the discharging state **SwitchCharging** is set to 0, preventing further charging, and **SwitchLoad** is set to 1, allowing the current to flow through the load.
If any type of fault is detected, such as over-current, over-voltage, or under-voltage, while the **FaultCounter** is below the threshold of 5, the system transits to the **FaultOperation** state. Within this state, if an over-voltage or over-current error is detected while the battery is charging, the system responds by stopping the charging process, whereas if an under-voltage or over-current error is detected while the battery is discharging, the load is disconnected preventing further discharge.
The last state, **PermanentFault**, represents a critical condition where the system has encountered severe or repeated faults, as indicated by either a high **FaultCounter** value (equal to 5) or temperature-related errors, over-temperature or under-temperature. Transiting to this state, both the two switches are permanently set to 0, effectively disconnecting both the charging circuit and the load. This action is a protective measure to prevent any further damage to the battery or the system.

Chapter 4

Testing and Results

4.1 Testing on the Battery Pack

The first step in the simulations performed on the model is to test the correct functioning of the battery pack, focusing on its fundamental parameters, which include capacity, voltage, and current. This ensures that the battery pack meets the required specifications and performs reliably under expected operating conditions, confirming that it is ready for further use or integration into the system.

As mentioned in Chapter 3, the battery pack is configured in a 4p8s arrangement, which means that there are four cells connected in parallel and then eight of these parallel sets are grouped in series. This configuration yields a total capacity of 376 Ah. To verify the accuracy of this capacity, a small test circuit is assembled, including the battery and a Controlled Current Source, as depicted in Figure 4.1.

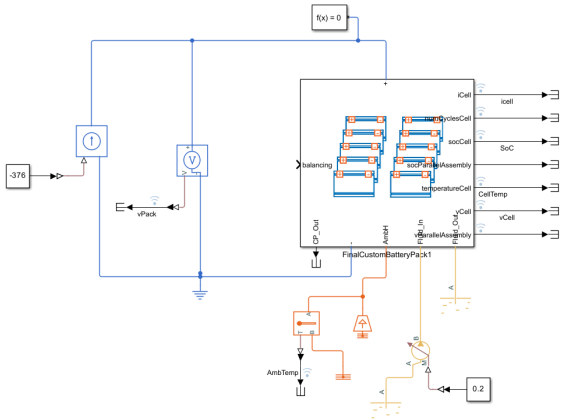

Figure 4.1: Simulink model of the Battery Pack capacity testing

In this setup, a Constant block with a value of -376 A is used as the input to the current source. The goal is to ensure that the battery discharges fully in exactly one hour, thereby confirming that the actual capacity matches the expected 376 Ah. Starting with a State of Charge set to 1 (100%), a one-hour simulation is conducted. Using the Data Inspector tool, the resulting SoC curve for the first cell, which is the same for the others, is illustrated in Figure 4.2.

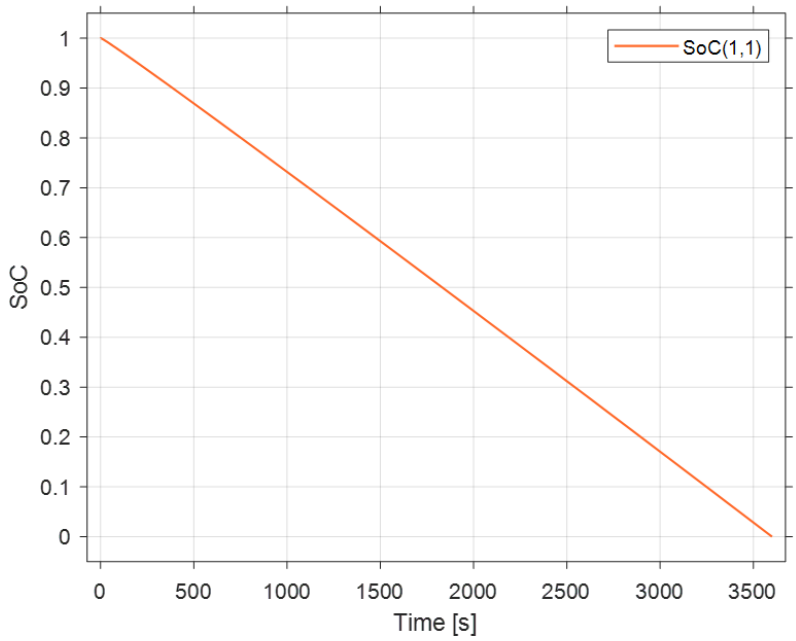

Figure 4.2: Battery Pack capacity testing results

Analyzing the test results, it is observed that, as expected, the SoC of the cell decreases to 0 precisely after 3600 seconds (1 hour). This outcome confirms that the capacity of the battery pack is exactly 376 Ah.

Continuing with the simulations, another simple test circuit is implemented by placing a Resistor in series with the battery pack and a Voltage Sensor in parallel, as shown in Figure 4.3.
In this configuration, a resistance value of 0.1 Ω is selected. This setup allows for a controlled discharge of the battery pack, providing an opportunity to closely monitor the voltage behavior. The results of the test are presented in Figure 4.4.

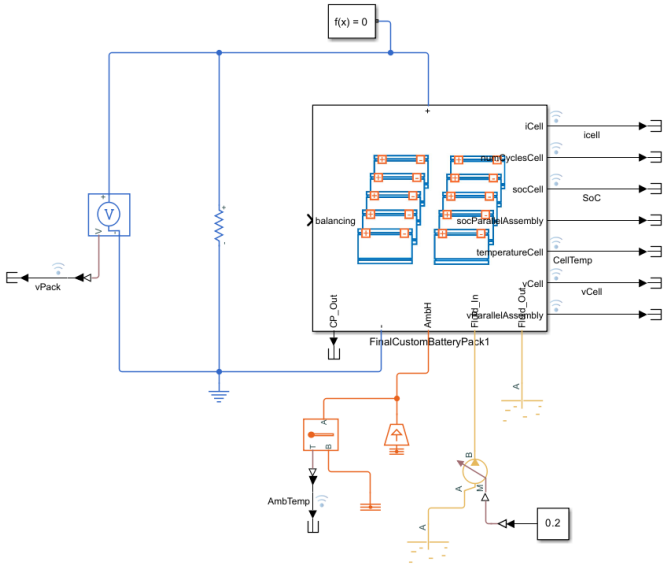

Figure 4.3: Simulink model of the Battery Pack voltage testing

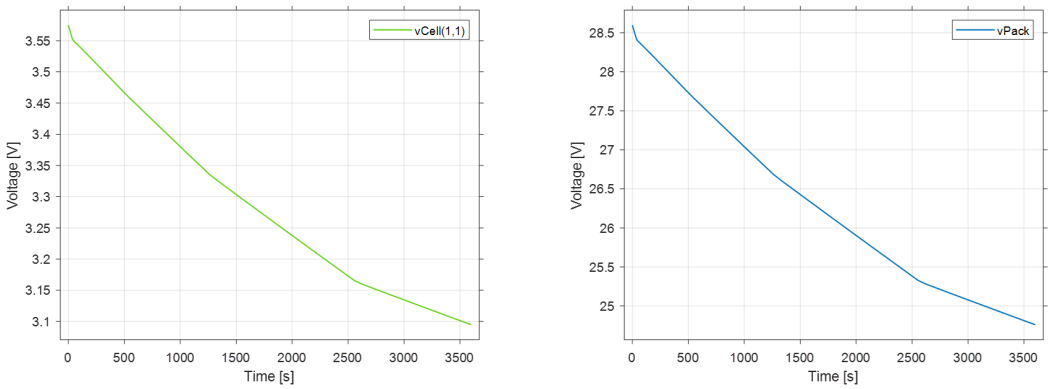

(a) Cell voltage results

(b) Battery Pack voltage results

Figure 4.4: Battery Pack voltage testing results

It can be observed the behavior of the voltage of the first cell, as shown in Figure 4.4a. The voltage of this cell is consistently around 3.6 V at t=0, which is the same across all cells, and then decreases over time. Additionally, Figure 4.4b illustrates the voltage of the entire battery pack, which is almost equal to 29 V at t=0, as anticipated based on the configuration and design of the battery system.

4.2 Charge and Discharge circuit

After completing the preliminary tests on the battery using basic testing circuits, a more sophisticated charge and discharge circuit is designed and implemented, as shown in Figure 4.5. This new circuit allows for a more detailed and accurate analysis of the battery parameters.

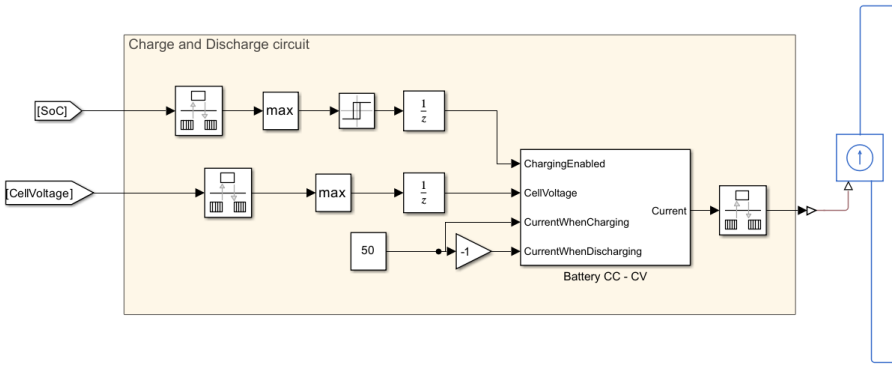

Figure 4.5: Charge and Discharge circuit Simulink model

In this configuration, the primary control unit is the Battery CC-CV block, which is responsible for executing the Constant Current Constant Voltage charging method. During the charging process, the system initially operates Constant Current (CC) mode, where the battery is charged at a steady predetermined current. This phase continues until the battery reaches a specified voltage level. Once this voltage threshold is achieved, the charging process transitions to Constant Voltage (CV) mode. In this mode, the voltage is maintained at a constant level, while the charging current gradually decreases as the battery approaches full charge.
The Battery CC-CV block takes in several inputs:

- The **ChargingEnabled** is a binary signal that dictates whether the battery charging process should be activated. When the signal is set to 1, the charging process is enabled, allowing current to flow into the battery to recharge it. In contrast, when the signal is set to 0, the charging process is disabled.
  This binary signal is generated by a Relay that takes as input the State of Charge of the most charged cell. Specifically, the relay operates based on two specific thresholds: the "Switch on point" and the "Switch off point". The first is set to a value of 0.9, meaning the charging process will be disabled when the SoC of the most charged cell reaches this threshold. On the other hand, the "Switch off point" is set to 0.3, indicating that the charging process will be enabled once the SoC of the most charged cell falls below this lower limit.

- The **CellVoltage** input port is designed to take as input the maximum voltage

value among all the individual cells within the battery pack. This approach ensures that the most critical cell, in terms of voltage, is used as a reference for monitoring and control purposes.

- The **CurrentWhenCharging** is a predefined constant set to a value of 50 A, which specifies the current that the battery uses during the charging process.

- The **CurrentWhenDischarging** refers to the electrical current utilized during the discharging process. In the configuration, it is set equal to -50 A.

Regarding the outputs, the final output of the Battery CC-CV block is the **Current**, which represents the actual current flowing through the battery, whether in charging or discharging mode.
Once generated by the Battery CC-CV block, this current is then fed into the external circuit connected to the battery via a Controlled Current Source. This controlled current source ensures that the exact amount of current calculated by the CC-CV block is accurately delivered to or drawn from the battery, enabling precise management of the charging and discharging processes.

4.3 Testing on SoC and SoH estimators

A series of simulations are carried out to practically evaluate the performance and accuracy of the State of Charge (SoC) and State of Health (SoH) estimators.
The first step in these simulations is to modify the initial value of the SoC of each parallel battery assembly. In particular, the SoC values are intentionally reduced, from the original value of 1, to simulate partially discharged battery states, which allows for testing the ability of the estimators to estimate the remaining charge under non-ideal conditions. The modified values of the initial SoC of each parallel assembly are collected in the Table 4.1:

ParallelAssembly	**Initial SoC value**
ParallelAssembly1	0.69
ParallelAssembly2	0.715
ParallelAssembly3	0.7
ParallelAssembly4	0.7
ParallelAssembly5	0.69
ParallelAssembly6	0.715
ParallelAssembly7	0.71
ParallelAssembly8	0.7

Table 4.1: Initial SoC values for each parallel assembly

Moving forward, the simulations have been conducted using two key models: the one illustrated in Figure 3.6, which provides a representation of the Simulink model of the SoC and SoH estimators, and the Charge and Discharge circuit model, which is described in section 4.2. The resultant Simulink model is illustrated in Figure 4.6.

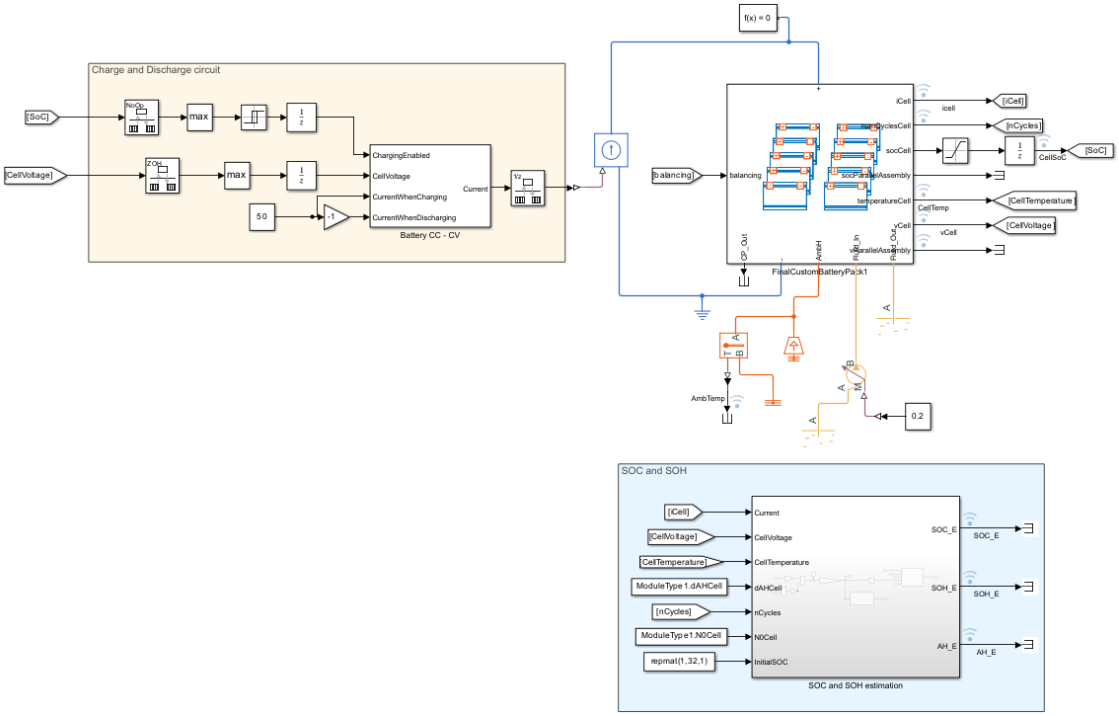

Figure 4.6: Simulink model for the testing of the SoC and SoH estimators

After configuring the simulation to run for a total duration of seven hours (2.52×10^4 seconds), the results are shown in Figure 4.7.
The simulation results for two cells, specifically the first and the fifth, are presented. The first cell, which belongs to the first parallel assembly, begins with an initial value of SoC of 0.69 (69%), whereas the fifth cell, which belongs to the second parallel assembly, has an initial value of 0.715 (71.5%). The SoC estimator block is initialized with a starting estimate of 1 (100%), and over approximately 500 seconds, the estimated SoC gradually converges to the actual SoC value. By the end of this period, the difference between the estimated and real SoC values is minimal, indicating that the estimator is functioning effectively.

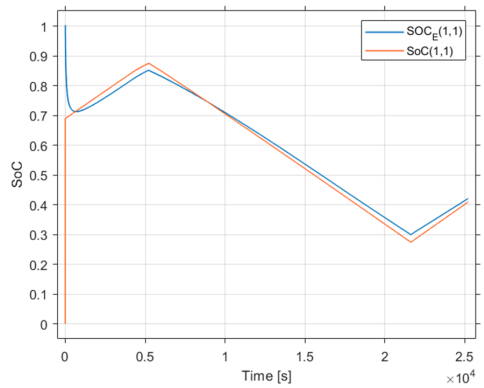

(a) SoC estimation of the first cell

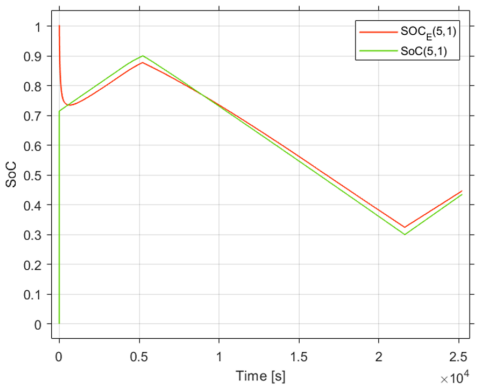

(b) SoC estimation of the fifth cell

Figure 4.7: SoC estimation testing results

Regarding the SoH estimation, the State of Health is strictly correlated to the capacity of the battery, as mentioned in section 3.1. Specifically, as the battery undergoes aging, its capacity gradually decreases, and this decline is directly reflected in the SoH metric. To illustrate this relationship, Figure 4.8 shows a comparison between the estimated capacity and the SoH of the first cell. It can be seen that as the capacity of the battery diminishes over time, the SoH metric follows a similar downward trend.

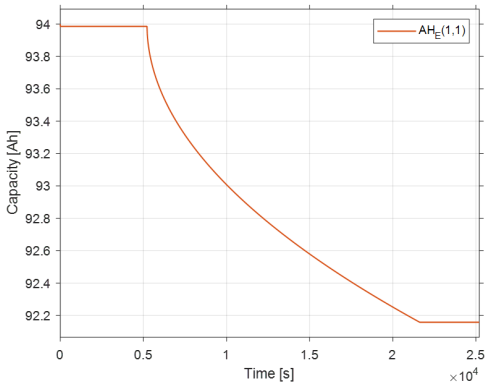

(a) Capacity estimation of the first cell

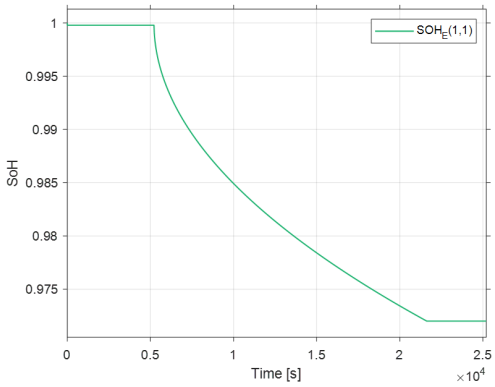

(b) SoH estimation of the first cell

Figure 4.8: Capacity and SoH estimation testing results

4.4 Testing on the Thermal Management

A series of simulations are conducted, starting with the same configurations used for the SoC and SoH estimators, particularly utilizing the same charge and discharge circuitry. These simulations are performed under two different conditions: one set without Thermal Management and another set with Thermal Management. By comparing the results from both scenarios, it becomes possible to evaluate the impact of Thermal Management on the overall performance of the system.
Figure 4.9 illustrates the temperature profile of the first cell, which is identical to the temperature profiles of the other cells, in the absence of Thermal Management.

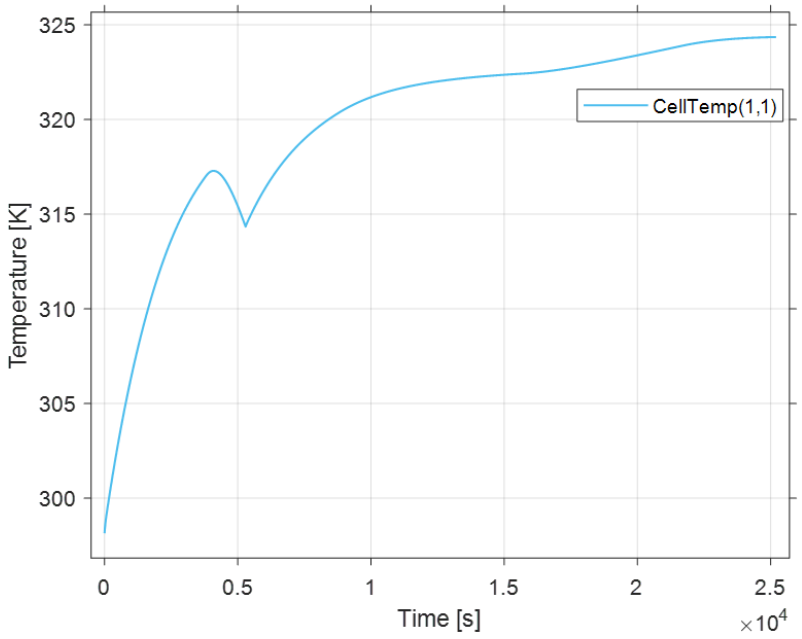

Figure 4.9: Temperature profile of the first cell in the absence of Thermal Management

As shown in the figure, the temperature, starting from an initial value of 298.15 K (the ambient temperature), increases during operation due to the lack of active cooling or heat dissipation mechanisms. This rise in temperature can cause significant thermal stress in the cell, potentially affecting its performance, efficiency, and overall useful life.
Additionally, it can be observed that the temperature decreases around 0.5×10^4 seconds. This happens during the charging phase, where the Battery CC-CV (Constant Current Constant Voltage) block is employed. Specifically, during the Constant Voltage (CV) mode, the current supplied to the battery gradually decreases as the cell approaches its fully charged state. As a result, the temperature

of the cell decreases too.

Continuing with the simulations, this time the Thermal Management system is activated, and the temperature profile of the first cell changes significantly, as shown in Figure 4.10.

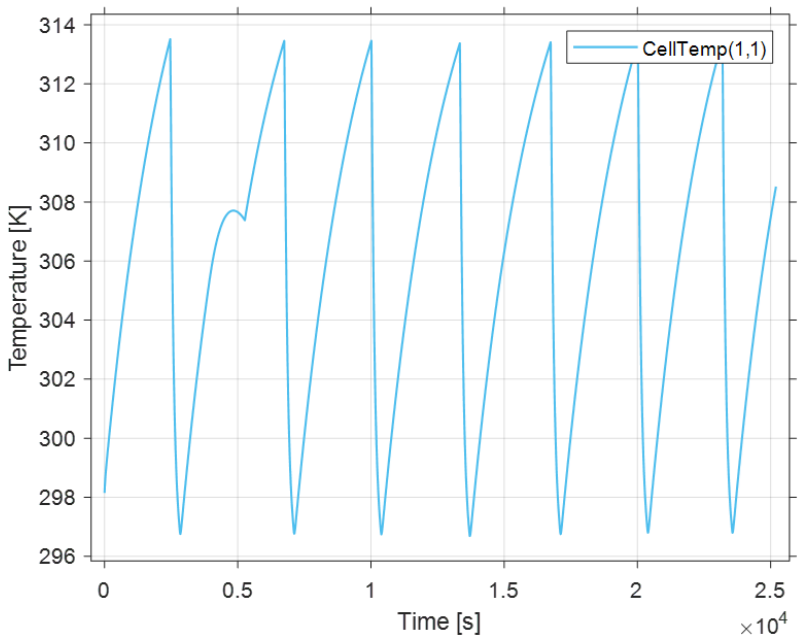

Figure 4.10: Temperature profile of the first cell in the presence of Thermal Management

It can be observed that the temperature of the cell, starting once again from an initial value of 298.15 K, gradually increases until it reaches the temperature of 313.15 K. At this point, the Thermal Management system is activated, triggering the flow of coolant through the battery. The activation of the Thermal Management is governed by the control strategy outlined in the Chart described in section 3.3. Once the system is triggered, the maximum coolant flow rate, which is equal to 0.5 kg/s, begins circulating through the battery, effectively dissipating the heat generated during operation.
As soon as the cell temperature decreases and reaches 306.15 K, the flow rate starts to gradually reduce. This is achieved through linear interpolation, where the flow rate decreases proportionally between the maximum value of 0.5 kg/s and the minimum flow rate of 0.2 kg/s, depending on the current temperature of the cell. Once the temperature drops below 298.15 K, the flow rate stabilizes at the minimum value of 0.2 kg/s, ensuring continuous but reduced cooling.
This flow rate behavior is depicted in Figure 4.11, with further detail provided in

Figure 4.11b, which offers a zoomed-in view of one specific instance of flow rate activation.

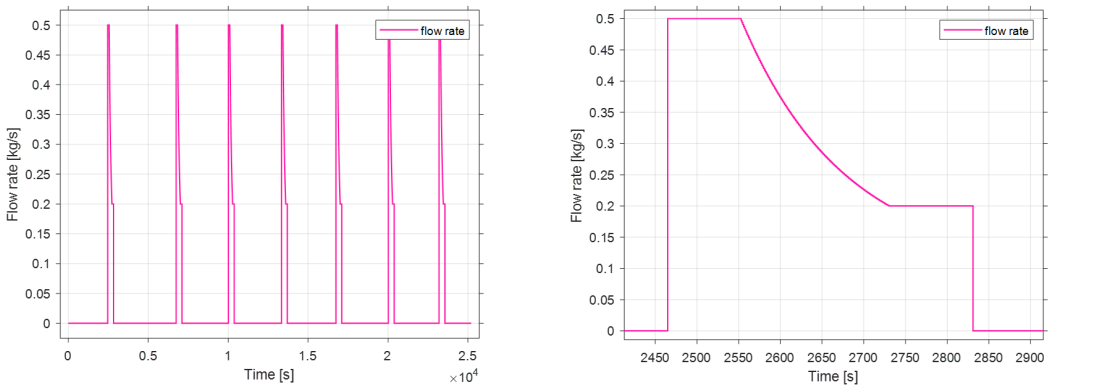

(a) Overall flow rate behavior

(b) Zoom in on one activation of the flow rate

Figure 4.11: Flow rate behavior

The figure highlights how the system transitions from the maximum flow rate of 0.5 kg/s to the minimum value of 0.2 kg/s, following the control strategy previously discussed. The zoomed section provides a clearer understanding of the dynamic of the system response to temperature changes, showcasing how the flow rate is finely tuned based on real-time temperature data.

4.5 Testing on the Passive Cell balancing

Using the same configuration as described in Section 3.4, together with the previously discussed charge and discharge circuit, the next step in testing the effectiveness of Passive Cell Balancing involves altering the initial State of Charge (SoC) of the cells. Specifically, the SoC values described in Table 4.1 are utilized to ensure consistency in the simulations. In addition, a simulation time of 12 hours (4.32×10^4 seconds) is used to better capture and highlight the behavior of the SoC.
Two different simulations are conducted for this purpose: one without the implementation of passive cell balancing and another with passive cell balancing enabled. The objective is to compare the behavior of the cells under both conditions and to evaluate the effectiveness of the balancing process in maintaining uniform SoC levels across the battery pack. The first simulation is shown in Figure 4.12.

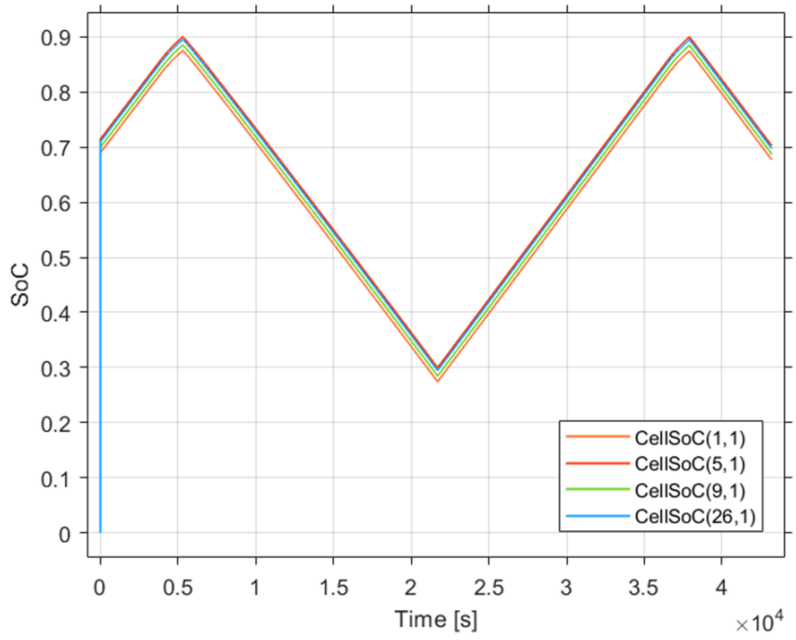

Figure 4.12: SoC behavior of cells without passive balancing

This simulation, which omits passive balancing, shows the behavior of four different cells, each with different initial SoC values. The purpose of this simulation is to establish a baseline to observe the natural divergence in the SoC of cells over time due to differences in their initial states. It can be clearly seen that the imbalance between cells remains constant throughout the simulation.

In the next phase of the experiment, Passive Cell balancing is activated to regulate the SoC across the same four cells. The behavior of these cells under the

influence of passive cell balance is illustrated in Figure 4.13.

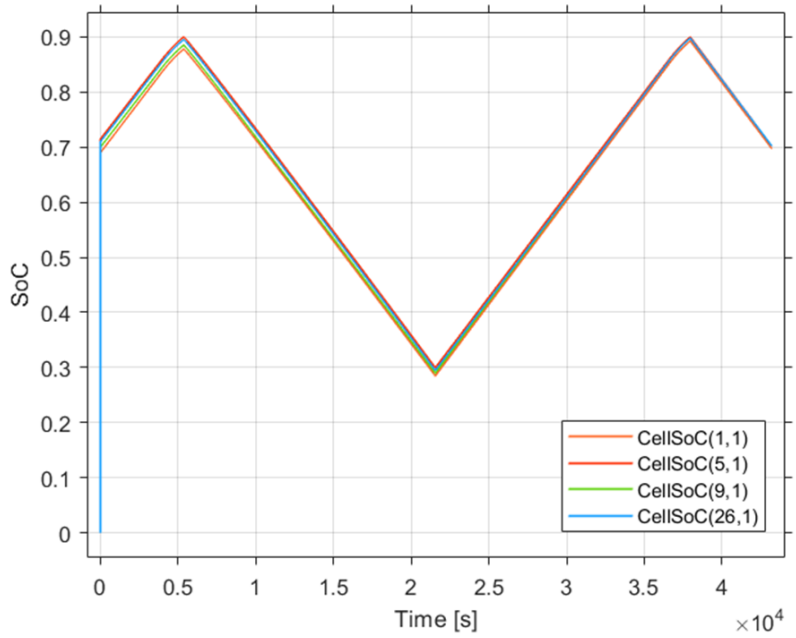

Figure 4.13: SoC behavior of cells with passive balancing

With the balancing mechanism engaged, the SoC of the cells begin to converge over time, in contrast to what observed in the previous simulation. This convergence demonstrates the effectiveness of passive balancing in equalizing differences between individual cells, ensuring a more uniform distribution of charge.
In conclusion, the model allows us to check the activation behavior of the passive cell balancing mechanism. It can be seen that the balancing process is immediately activated as the simulation starts because of differences in SoC among the cells. In the process, the system continues to balance the cells until these differences are minimized. Toward the end of the simulation, once the SoC levels converge and fall within acceptable limits, the passive cell balancing mechanism deactivates, indicating that equilibrium has been achieved.

4.6 Testing on the Fault Detection

The Fault Detection has the capability to identify various types of errors, such as those caused by over-current, under-temperature, over-temperature, under-voltage and over-voltage conditions. Several simulations are performed, each targeting different operational scenarios. The aim is to verify the proper functioning of the system under a wide range of possible fault conditions.
The initial simulations conducted focus on temperature-related faults, as these are the most critical. The first simulation is performed under normal conditions without introducing any faults. To maintain the temperature of cells within the safe operational limits ([270,320] K), the Thermal Management is integrated into the simulation. Performing a 12-hour simulation, the results are shown in Figure 4.14.

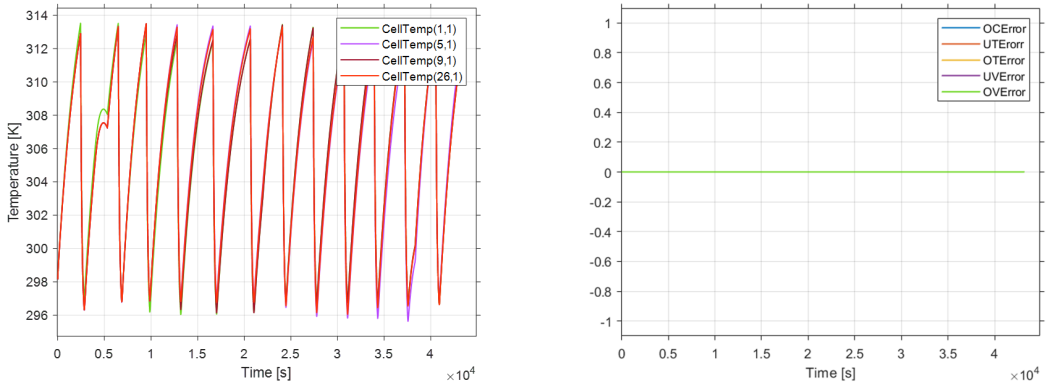

(a) Temperature profiles with the integration of Thermal Management

(b) Behavior of the error signals

Figure 4.14: Simulation results for the temperature-related faults

The left image, Figure 4.14a, illustrates the temperature profiles of four distinct battery cells. It is evident that each cell has a different temperature behavior, though all remain within the safety limits. These differences in temperature response are attributed to the varying initial SoC applied to each cell. In contrast, the right image, Figure 4.14b, shows the behavior of the error signals, all of which are all coincident and equal to zero, indicating that there are no faults.
Another important aspect to highlight is the behavior of the two switch signals dictated by the chart described in section 3.5. Figure 4.15 presents a comparison between the SoC profile of the first cell and the activation of the two switch signals.

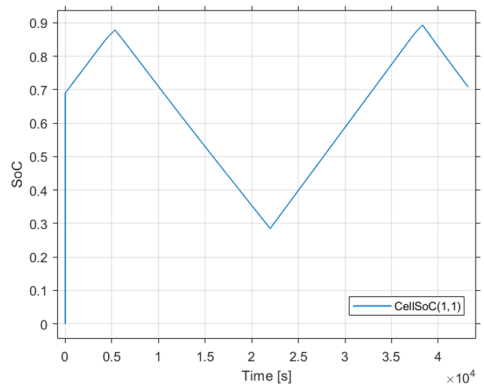

(a) SoC behavior of the first cell

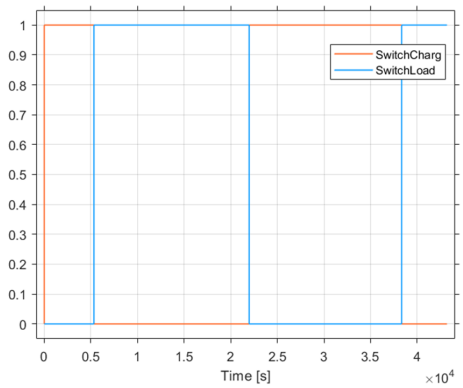

(b) Behavior of the two switch signals

Figure 4.15: Simulation results for the correct functioning of the Chart

As shown, when the cell is in recharging mode, indicated by an increase in the SoC, the charging switch signal is set to 1, enabling the battery to charge, while the load switch signal is set to 0, disconnecting the load. In contrast, when the SoC decreases, the cell is in the discharging state, the charging switch signal is set to 0, and the load switch is set to 1, allowing the current to flow through the load.

Following the initial testing, deliberate temperature errors are introduced to verify the correct response of the system. Specifically, the Thermal Management is disabled, causing the temperature of the battery cells to rise above the designed safe upper limit. The results of the simulation are depicted in Figure 4.16.

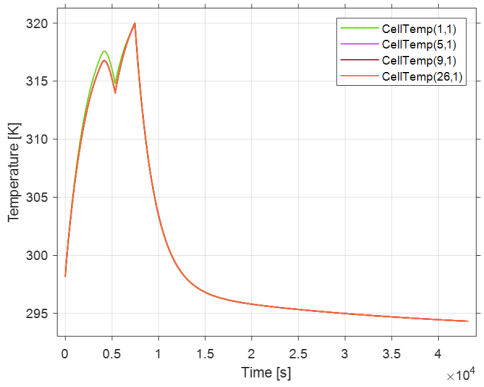

(a) Temperature profiles without the Thermal Management

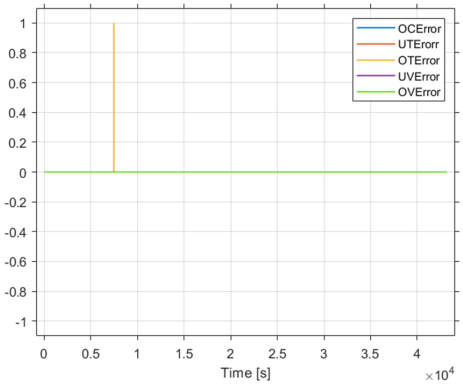

(b) Behavior of the error signals with the over-temperature fault

Figure 4.16: Simulation results for the detection of the over-temperature fault

In this simulation scenario, the temperature of the cells is allowed to increase unchecked until it reaches the critical upper limit of 320 K. This temperature rise occurs after approximately 2 hours (corresponding to 0.75×10^4 seconds of simulation time). Figure 4.16b clearly show that once the cell temperature reaches this threshold, the system promptly detects the over-temperature condition. In particular, at this point, the Fault Detection triggers an over-temperature error, effectively disconnecting the battery from the circuit, preventing any potential damage to the battery cells.

Further confirmation of the accurate detection of the over-temperature fault is highlighted in Figure 4.17. This figure once again illustrates the comparison of the SoC of the first cell and the behavior of the two switch signals.

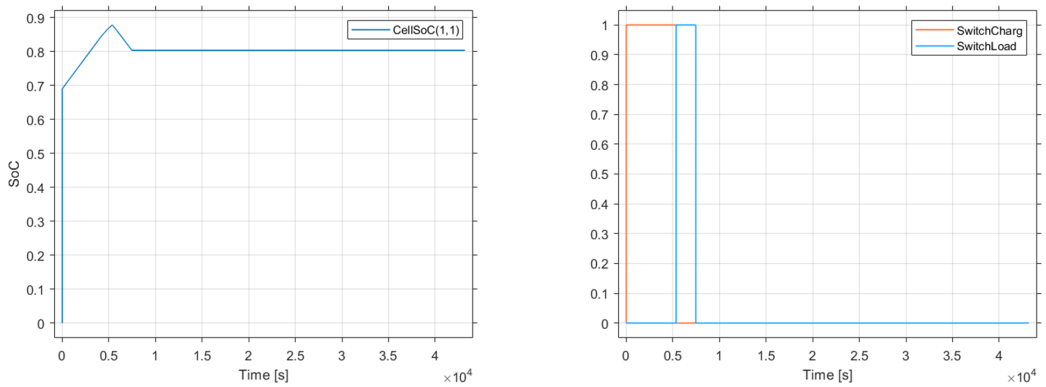

(a) SoC behavior of the first cell with over-temperature fault

(b) Behavior of the two switch signals with the over-temperature fault

Figure 4.17: Simulation results for the functioning of the Chart when there is an over-temperature fault

As shown, while the cell is discharging, indicated by a decrease in the SoC, the load switch signal is set to 1, and the charging switch load is set to 0. The moment the cell temperature exceeds the safety limit and the over-temperature fault is detected, both signals transition to their off-state, effectively isolating the battery from the circuit.

Another significant error is the over-current error. To simulate this type of error, a variable resistor is introduced in the circuit to serve as the load, substituting the original fixed resistor. This variable resistor assumes two different resistance values: 0.6 Ω and 0.4 Ω. When the resistance is set to 0.6 Ω, the current flowing through the battery is approximately -52 A. However, when the resistance is decreased to 0.4 Ω, the current increases, in absolute value, to around -76 A.

This latter value exceeds the predefined over-current threshold of -72 A, triggering the over-current protection mechanism. Figures 4.18 and 4.19 illustrate: on the left, the error signals, which shows when the over-current error is detected; on the right, the corresponding behavior of the current is shown as the resistance changes, highlighting the point at which the current surpasses the safety threshold.

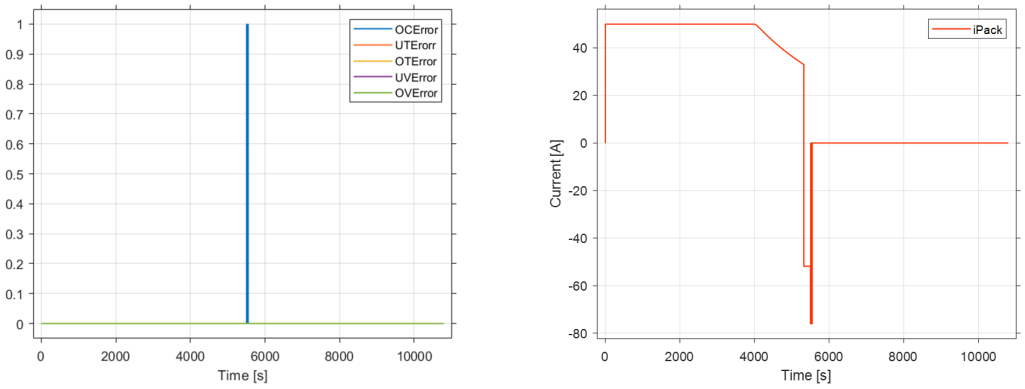

(a) Behavior of the error signals with the over-current fault

(b) Behavior of the current flowing through the pack

Figure 4.18: Simulation results for the detection of the over-current fault

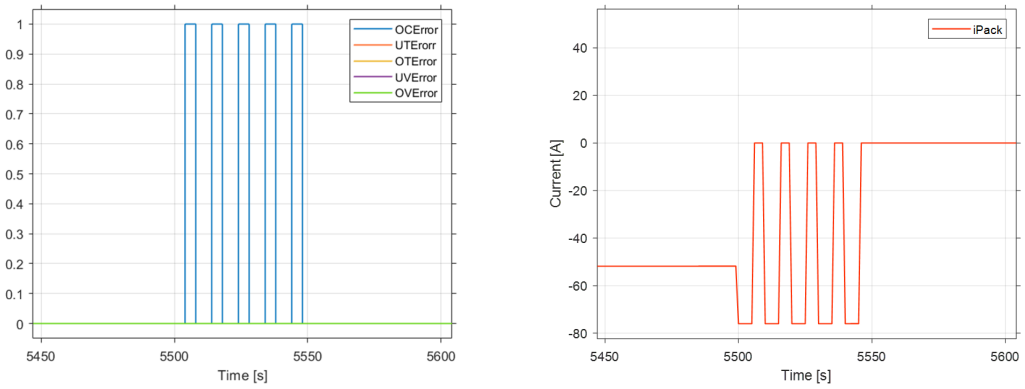

(a) Zoom in on the behavior of the error signals with the over-current fault

(b) Zoom in on the behavior of the two switch signals with the over-temperature fault

Figure 4.19: Zoom in on the simulation results for the functioning of the Chart when there is an over-current fault

Referring to Figure 4.19a, it is evident that once the system detects five consecutive over-current errors, the battery pack is disconnected from the circuit to prevent

potential damage to the battery. Simultaneously, the current flowing through the battery pack drops from -76 A to 0 A each time the load switch opens. After five consecutive over-current detection, the switch remains open and the current is held at 0 A to ensure no further current flows through the pack.
This behavior of the system is further highlighted in Figure 4.20, which depicts the operation of the two switches responsible for connecting and disconnecting the charging circuit and the load.

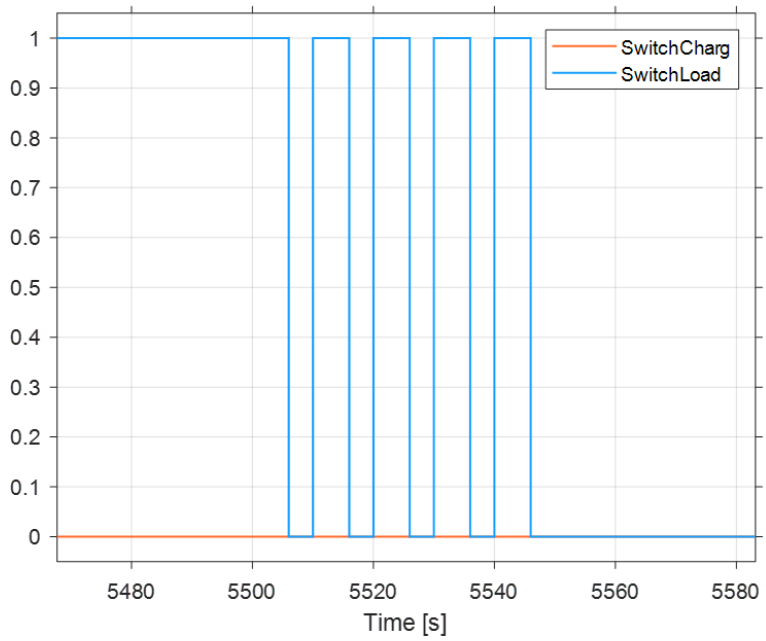

Figure 4.20: Behavior of the two switch signals with the over-current fault

The final set of simulations has the goal of inducing an over-voltage error in the system. To do so, the original circuit to which the battery is connected has been modified. In particular, a DC voltage source has been added to the branch that contains the resistor and the switching load. The purpose of this voltage source is to increase the voltage of the battery pack, overcoming the maximum threshold, thereby simulating an over-voltage condition.
The results of the simulations are illustrated in Figures 4.21 and 4.22. On the left is shown the behavior of the error signals, and on the right is the voltage profile of the fifth cell in the battery pack.

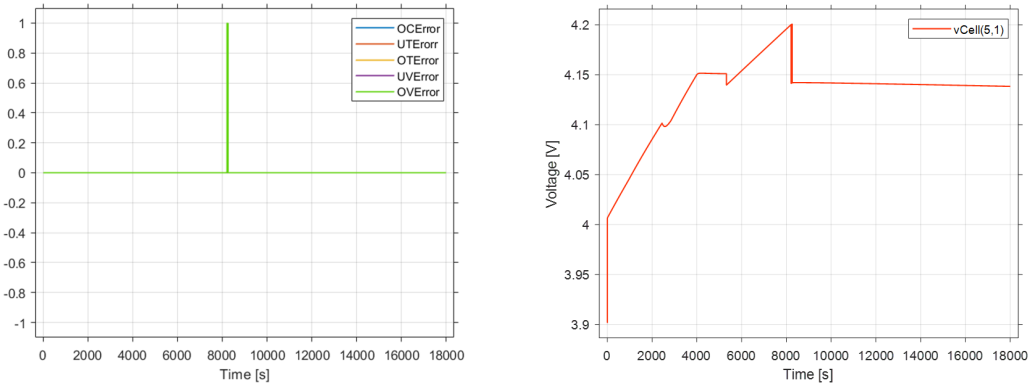

(a) Behavior of the error signals with the over-voltage fault

(b) Behavior of the cell voltage with the over-voltage fault

Figure 4.21: Simulation results for the detection of the over-voltage fault

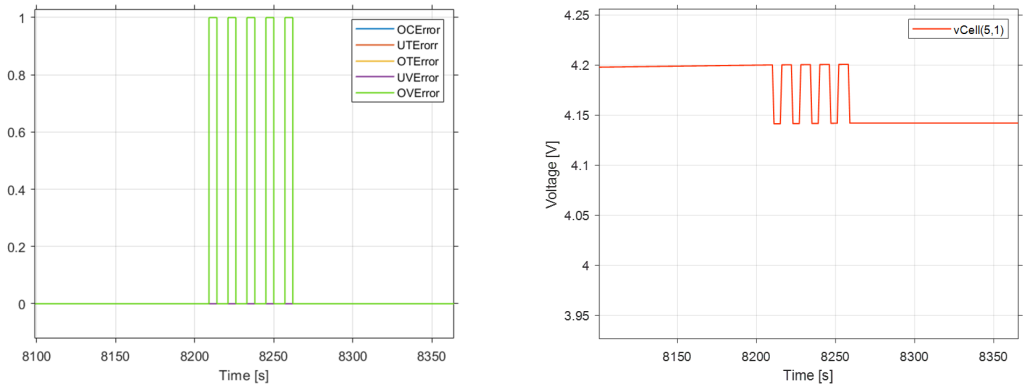

(a) Zoom in on the behavior of the error signals with the over-voltage fault

(b) Zoom in on the behavior of the cell voltage with the over-voltage fault

Figure 4.22: Zoom in on the simulation results for the detection of the over-voltage fault

It is evident that as soon as the voltage of the cell reaches the upper limit, which is set at 4.2 V, the system promptly identifies the over-voltage error. Furthermore, if five consecutive over-voltage errors are detected, the BMS responses by disconnecting immediately the battery pack from the circuit. This mechanism highlights robust error-detection and protective capabilities of the BMS in maintaining safe battery operation under abnormal conditions.

4.7 Testing on the complete model

In conclusion, several simulations are performed on the complete model to verify whether each function works properly while all are active, avoiding any type of errors. These simulations employ the Charge and Discharge circuit, as described in Section 4.2. In addition, a variable resistor has been used, which is configured to alternate between two different resistance values: 0.8 Ω and 0.5 Ω. This approach allows to simulate a dynamic load condition, representing a system that demands varying current levels.
The described Simulink model used for these simulations is depicted in Figure 4.23.

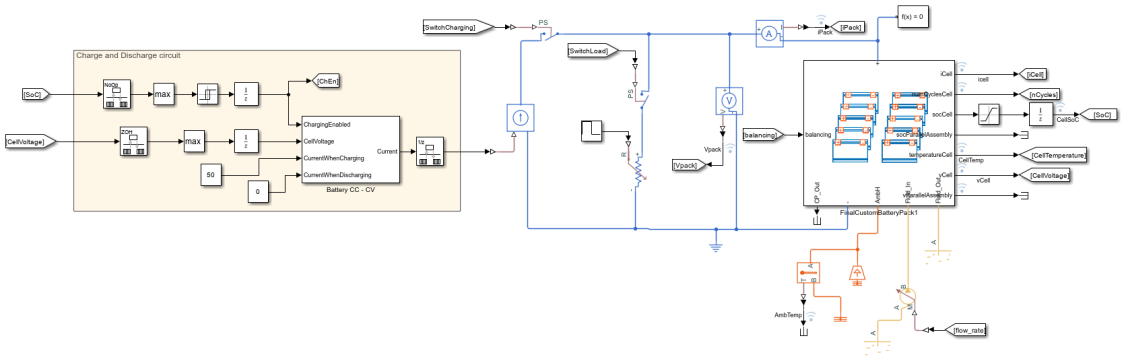

Figure 4.23: Simulink model for final testing

By conducting a twelve-hours simulation, the resulting profiles for both the current flowing through the battery pack and the State of Charge (SoC) of four individual cells are illustrated in Figure 4.24.

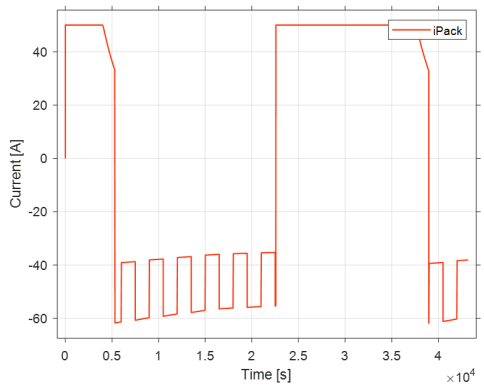

(a) Behavior of the current flowing through the battery pack

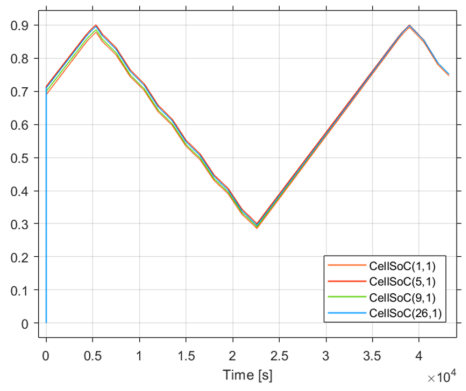

(b) SoC behavior of cells

Figure 4.24: Simulation results of the complete model

Focusing on Figure 4.24a, after the initial phase of charging at constant current, the current profile highlights the fluctuations in power demand as soon as the load is connected. These variations are caused by the presence of the variable resistor and the ability of the system to respond to the changing load.
Regarding the SoC behavior, it is evident that, during the discharging phase, it no longer follows a linear trajectory. Instead of maintaining a steady decline, the SoC profile is influenced by the dynamic load conditions and the response of the system to fluctuating current demands. Furthermore, Figure 4.24b clearly shows the proper functioning of the passive cell balancing mechanism. By the end of the simulation, the SoC of the four individual cells converges to the same value.

In addition, the simulation results shown in Figure 4.25 clearly demonstrate that the temperature profiles remains within the defined threshold limits. This means that the Thermal Management is working properly, effectively preventing overheating.

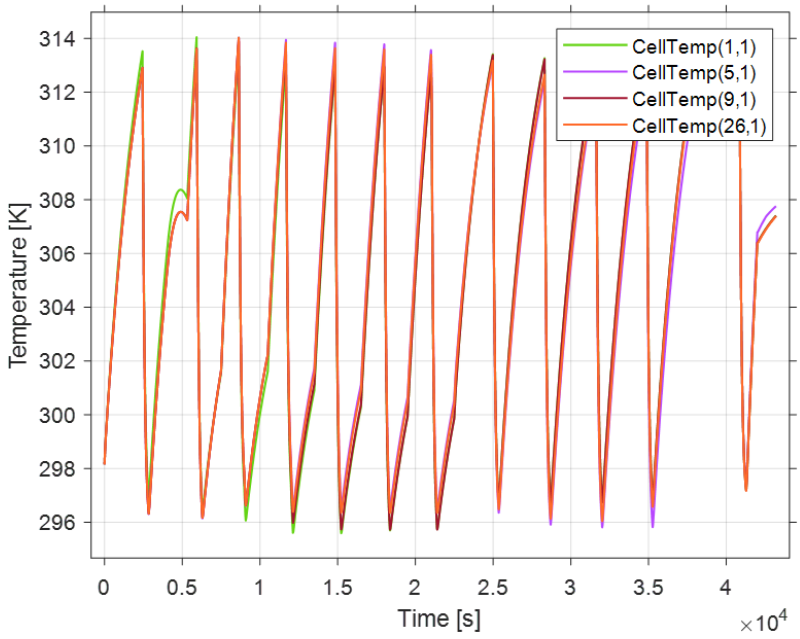

Figure 4.25: Temperature profile of four individual cells

Moving forward, Figure 4.26, illustrates that the State of Charge estimator is also capable to varying current demands. The SoC estimator tracks the real-time SoC behavior of the cell.

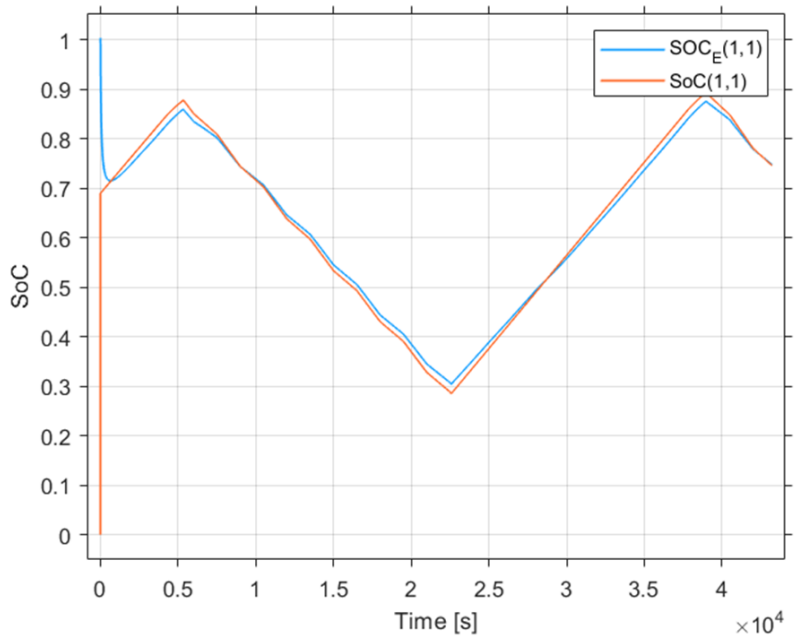

Figure 4.26: SoC estimation testing result of the complete model

Finally, Figure 4.27 presents two important aspects: the estimated capacity of the battery on the left, and the State of Health on the right. As anticipated, as the capacity of the battery decreases over time, the SoH follows the same trend, reflecting the natural degradation of the battery.

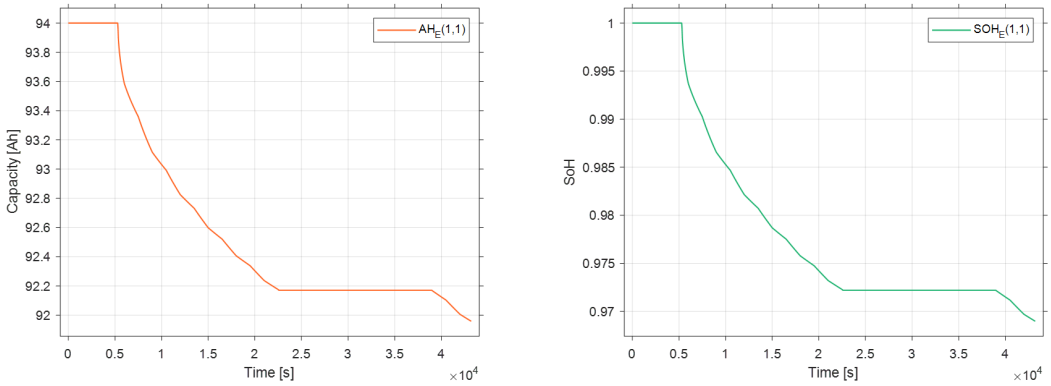

(a) Capacity estimation of the first cell

(b) SoH estimation of the first cells

Figure 4.27: Capacity and SoH estimation results of the complete model

Chapter 5

Conclusions and Future Works

5.1 Conclusions

This thesis aimed to develop a Battery Management System (BMS) capable of efficiently managing battery charge, monitoring health conditions, detecting potential errors, and evaluating the impact of thermal management on system performance.
Initially, the research began by exploring theoretical foundations to understand the implementation strategy of the BMS functions. The thesis starts by providing a detailed overview of the battery technologies commonly used in the automotive sector. Specifically, key parameters, such as capacity, energy capacity, energy density, power density, and cycle life, are thoroughly explained to establish a solid understanding of battery performance metrics. Additionally, the various chemical compositions of batteries have been presented, including lead-acid, nickel-cadmium, sodium-nickel chloride, and lithium-ion, highlighting their advantages and limitations. The research also examines the shapes of cells, such as cylindrical, prismatic, and pouch cells in order to have a perspective on the range of design solutions available.
Furthermore, in this work has been illustrated the key concepts of the ISO 26262 standard, which governs functional safety. It has been analyzed the first four parts of the standard, which highlight essential elements such as hazard analysis, risk assessment, and the assignment of Automotive Safety Integrity Levels (ASIL), which are crucial for evaluating the safety requirements of a BMS.
Proceeding further, the core functions of a BMS were thoroughly examined and implemented in the model, including State of Charge (SoC) and State of Health (SoH) estimations, Cell balancing, Thermal Management, and Fault Detection. Each function was described in detail, focusing on the various methods and techniques used to implement them.
For instance, in the case of SoC and SoH estimation, the Unscented Kalman Filter (UKF) was employed. This method represents an improved version of

the traditional Kalman Filter (KF), offering improved accuracy in estimating nonlinear system states. Regarding the cell balancing, it has been chosen the passive cell balancing. This method allows to dissipate excess energy from more charged cells through resistive elements to equalize the State of Charge (SoC) of cells among the battery pack. For thermal management, an active cooling system was implemented. The last one can regulate the coolant flow rate depending on the temperature of the cells to maintain optimal operating temperatures.

Subsequently, several simulations of the implemented model were conducted to verify the correct functioning of each individual component as well as the complete model. Specifically, the simulations were designed to test both the fundamental parameters of the battery pack and the performance of each core function within the system. Initially, tests were focused on the basic characteristics of the battery, such as capacity, voltage, and current. Following this, simulations to evaluate the performance of each specific BMS function were carried out. Each function was subjected to a variety of simulation setups to ensure that it operated as expected, such as varying load, charge/discharge cycles, and temperature fluctuations.
Finally, several simulations were conducted to verify the proper functioning of the BMS under a wide range of possible fault conditions. The goal of these tests was to intentionally induce different types of faults, such as over-temperature, over-voltage and over-current, in order to verify the response of the system. In particular, these fault conditions were simulated to ensure that the BMS is capable of detecting anomalies promptly and isolating the battery pack from the circuit to prevent it from possible damage.

In conclusion, following the various simulations carried out, it was evident that the implemented Battery Management System (BMS) demonstrates the ability to effectively manage the battery pack. Specifically, the BMS can:

- Accurately estimate both the State of Charge (SoC) and the State of Health (SoH) of the battery pack.

- Effectively control the temperature of the cells, preventing overheating.

- Balance the SoC across individual cells, ensuring a more uniform charge distribution.

- Quickly detect fault conditions and protect the battery pack by disconnecting it from the circuit.

5.2 Future Works

This thesis has demonstrated the importance and role of a Battery Management System (BMS) in managing the battery pack throughout its operational life. In particular, the BMS ensures the safety, reliability, and efficiency of the battery system.
A possible consequent future work could involve the integration of a heater control unit into the current model. This system would be capable of warming the battery pack when the temperature falls below a predefined threshold, addressing the challenges of operating in colder environments. In fact, in the present model, this functionality was not included, as it was assumed that the ambient temperature remained consistently around 298.15 K (25 °C).
Another possible line of research is to test the BMS model and the battery pack with a real load. In fact, in the current simulations, a resistive load was used to represent the power demand, which simplifies the system but may not capture the complexity of the actual operating conditions. An example can be to test the system with an electric motor. By doing so, the system could be subjected to variable power demands and dynamic current draw, which allows the simulation of the behavior of the battery in real applications.
Finally, another promising avenue for future research is the integration of the requirements outlined in ISO 26262. The integration of the standard into the design and validation of BMS will be able to enhance the safety of the system in such a way that it can extend the applicability of the system into the automotive domain, where functional safety becomes very crucial. This approach requires a detailed hazard analysis and risk assessment, specification of safety goals, and realization of the required safety mechanisms necessary for the prevention/mitigation of failures leading to unsafe conditions. In addition to improving the reliability of the BMS, the integration of functional safety will ensure compliance with industry standards.

Bibliography

[1] K. LIU, K. LI, Q. PENG, and C. ZHANG, "A brief review on key technologies in the battery management system of electric vehicles," *Front. Mech. Eng. 14*, p. 47–64, 2019. [Online]. Available: https://link.springer.com/article/10.1007/s11465-018-0516-8

[2] Dickson, Hannan, H. Lipu, and P. J. Ker, "State of charge estimation for lithium-ion batteries using model-based and data-driven methods: A review," *IEEE Access*, vol. vol. 7, pp. 136 116–136 136, 2019. [Online]. Available: https://ieeexplore.ieee.org/abstract/document/8843918

[3] Evlithium. Samsung sdi 3.7v 94ah nmc prismatic battery cell. [Online]. Available: https://www.evlithium.com/nmc-battery/samsung-sdi94-94ah-nmc-battery.html

[4] Uzair, Abbas, and Hosain, "Characteristics of battery management systems of electric vehicles with consideration of the active and passive cell balancing process," *World Electric Vehicle Journal*, vol. 12, no. 3, 2021. [Online]. Available: https://www.mdpi.com/2032-6653/12/3/120

[5] Ntombela, Mlungisi, K. Musasa, and K. Moloi, "A comprehensive review for battery electric vehicles (bev) drive circuits technology, operations, and challenges," *World Electric Vehicle Journal 14, no. 7: 195*, vol. 14, no. 7, 2023. [Online]. Available: https://www.mdpi.com/2032-6653/14/7/195

[6] A. Khaligh and Z. Li, "Battery, ultracapacitor, fuel cell, and hybrid energy storage systems for electric, hybrid electric, fuel cell, and plug-in hybrid electric vehicles: State of the art," *IEEE Transactions on Vehicular Technology*, vol. 59 no. 6, pp. 2806–2814, 2010. [Online]. Available: https://ieeexplore.ieee.org/abstract/document/5446335

[7] I. Baccouche, A. Mlayah, S. Jemmali, B. Manai, and N. Essoukri Ben Amara, "Implementation of a coulomb counting algorithm for soc estimation of li-ion battery for multimedia applications," *2015 IEEE 12th International Multi-Conference on Systems, Signals & Devices (SSD15), Mahdia, Tunisia*, pp. 1–6, 2015. [Online]. Available: https://ieeexplore.ieee.org/abstract/document/7348255

[8] I. O. for Standardization, "Iso 26262: Road vehicles – functional safety," International Organization for Standardization, Geneva, Switzerland, Tech. Rep.,

2018.

[9] J. Dawson and D. Garikapati, "Extending iso26262 to an operationally complex system," *2021 IEEE International Systems Conference (SysCon), Vancouver, BC, Canada*, pp. 1–7, 2021. [Online]. Available: https://ieeexplore.ieee.org/document/9447146

[10] BYHON. Iso 26262 asil: cos'è l'automotive safety integrity level. [Online]. Available: https://www.byhon.it/it/iso-26262-asil-cose-lautomotive-safety-integrity-level/

[11] H. Rahimi-Eichi, U. Ojha, F. Baronti, and M. Y. Chow, "Battery management system: An overview of its application in the smart grid and electric vehicles," *IEEE Industrial Electronics Magazine*, vol. vol. 7, no. 2, pp. 4–16, 2013. [Online]. Available: https://ieeexplore.ieee.org/abstract/document/6532486

[12] I. N. Haq, E. Leksono, M. Iqbal, F. X. N. Sodami, Nugraha, D. Kurniadi, and B. Yuliarto, "Development of battery management system for cell monitoring and protection," *International Conference on Electrical Engineering and Computer Science (ICEECS), Kuta, Bali, Indonesia*, pp. 203–208, 2014. [Online]. Available: https://ieeexplore.ieee.org/abstract/document/7045246

[13] M. Murnane and A. Ghazel, "A closer look at state of charge (soc) and state of health (soh) estimation techniques for batteries," *Analog Devices*, 2023. [Online]. Available: https://www.analog.com/en/resources/technical-articles/a-closer-look-at-state-of-charge-and-state-health-estimation-tech.html

[14] J. Tao, S. Wang, W. Cao, P. Takyi-Aninakwa, C. Fernandez, and J. M. Guerrero4, "A comprehensive review of state-of-charge and state-of-health estimation for lithium-ion battery energy storage systems," *Ionics*, 2024. [Online]. Available: https://link.springer.com/article/10.1007/s11581-024-05686-z

[15] S. Barcellona and L. Piegari, "Lithium ion battery models and parameter identification techniques," *Energies*, 2017. [Online]. Available: https://www.mdpi.com/1996-1073/10/12/2007

[16] C. Lin, A. Tang, and W. Wang, "A review of soh estimation methods in lithium-ion batteries for electric vehicle applications," *Energy Procedia*, vol. vol. 75, pp. 1920–1925, 2019. [Online]. Available: https://www.sciencedirect.com/science/article/pii/S1876610215009674

[17] L. Ungurean, G. Cârstoiu, M. V. Micea, and V. Groza, "Battery state of health estimation: a structured reviewof models, methods and commercial devices," *International journal of Energy Research*, pp. 151–176, 2016.

[18] B. Balagopal and M. Y. Chow, "The state of the art approaches to estimate the state of health (soh) and state of function (sof) of lithium ion batteries," *IEEE 13th International Conference on Industrial Informatics (INDIN), Cambridge, UK*, pp. 1302–1307, 2015. [Online]. Available: https://ieeexplore.ieee.org/abstract/document/7281923/authors#authors

[19] S. K. Pradhan and B. Chakraborty, "Battery management strategies:

An essential review for battery state of health monitoring techniques," *Journal of Energy Storage*, vol. 51, 2022. [Online]. Available: https://www.sciencedirect.com/science/article/pii/S2352152X22004509

[20] T. Wu, F. J. L. Liao, and C. Chang, "Voltage-soc balancing control scheme for series-connected lithium-ion battery packs," *Journal of Energy Storage*, vol. 25, 2019. [Online]. Available: https://www.sciencedirect.com/science/article/pii/S2352152X19305080

[21] MathWorks, *MATLAB*, MathWorks, 2023. [Online]. Available: https://www.mathworks.com/products/matlab.html

[22] MATLAB. Tabulated battery model. [Online]. Available: https://it.mathworks.com/help/sps/ref/batterytablebased.html

[23] W. He, N. Williard, C. Chen, and M. Pecht, "State of charge estimation for electric vehicle batteries using unscented kalman filtering," *Microelectronics Reliability*, vol. 53, Issue 6, pp. 840–847, 2013. [Online]. Available: https://www.sciencedirect.com/science/article/pii/S0026271412005185

[24] I. Jokic, Z. Zecevic, and B. Krstajic, "State-of-charge estimation of lithium-ion batteries using extended kalman filter and unscented kalman filter," *2018 23rd International Scientific-Professional Conference on Information Technology (IT)*, pp. 1–4, 2018. [Online]. Available: https://ieeexplore.ieee.org/abstract/document/8350462

[25] W. Wang, X. Wang, C. Xiang, C. Wei, and Y. Zhao, "Unscented kalman filter-based battery soc estimation and peak power prediction method for power distribution of hybrid electric vehicles," *IEEE Access*, vol. 6, pp. 35 957–35 965, 2018.